A NEW METHOD OF CORRECTION SIGNAL DAMPING

Charles R. Smith, Jr.
and
Samuel F. Powel, III

A NEW METHOD OF CORRECTION SIGNAL DAMPING

by

CHARLES R. SMITH, JR., Lieutenant, U.S. Navy
B.S., U.S. Naval Academy, 1949
B.S., U.S. Naval Postgraduate School, 1956

SAMUEL F. POWEL, III, Lieutenant, U.S. Navy
B.S., U.S. Naval Academy, 1950
B.S., U.S. Naval Postgraduate School, 1956

SUBMITTED IN PARTIAL FULFILLMENT OF THE
REQUIREMENTS FOR THE DEGREE OF
MASTER OF SCIENCE
at the
MASSACHUSETTS INSTITUTE OF TECHNOLOGY
May, 1957

This thesis, written by the authors while affiliated with the Instrumentation Laboratory, M.I.T., has been reproduced by the offset process using printer's ink in accordance with the following basic authorization received by Dr. C. S. Draper, Head of Department of Aeronautical Engineering and Director of the Instrumentation Laboratory.

COPY

March 1, 1956

Dr. C. S. Draper
Head of the Department of Aeronautical Engineering
and Director of the Instrumentation Laboratory

Dear Dr. Draper:

This is to authorize the deposit in the Library of permanent, offset-printed copies of theses published by the Instrumentation Laboratory in lieu of the ribbon copies normally required.

A NEW METHOD OF CORRECTION SIGNAL DAMPING

by

Charles R. Smith, Jr.
Samuel F. Powel, III

Submitted to the Department of Aeronautical Engineering on May 20, 1957, in partial fulfillment of the requirements for the degree of Master of Science.

ABSTRACT

A new method of correction signal damping for direct-drive stable platforms was suggested by Lees. The method uses the correction signal voltage from the integrating gyro, differentiates the signal in a high-speed, second-order servomechanism, and adds the differentiated signal to the servo loop of the stable platform for damping.

In order to verify the theory an analog computer study was performed on such a system. In addition, a damping servomechanism was constructed and installed to damp an existing direct-drive stable platform. This investigation presents the results of testing the stable platform with damping servomechanism and compares these results to those results obtained from the analog computer study. Correlation between the results was observed, and the new method of correction signal damping was successful for the direct-drive stable platform tested.

Thesis Supervisor:	Sidney Lees
Title:	Assistant Professor of Aeronautical Engineering

ACKNOWLEDGEMENT

The authors wish to express their appreciation to the personnel of the Instrumentation Laboratory, Massachusetts Institute of Technology, who assisted in the preparation of this thesis. Particular thanks are due to Professor Sidney Lees who as thesis supervisor inspired and guided the investigation, Mr. L. R. Grohe, for making the test equipment available, and Mr. Andrew Lattanzi and his staff of technicians in the Miniature Components Laboratory, for their help in the technical aspects of the investigation.

The graduate work for which this thesis is a partial requirement was performed while the authors were attached to the U. S. Naval Administrative Unit, Massachusetts Institute of Technology.

TABLE OF CONTENTS

LIST OF ILLUSTRATIONS

OBJECT

The object of this investigation is to test experimentally a new method of correction signal damping applicable to stable platforms.

CHAPTER 1

INTRODUCTION

One of the major problems associated with the design and operation of stable platforms is to obtain effective damping without introducing into the system additional interferences, due to the motion of the vehicle in which the stable platform is carried, and thereby increasing the tracking error of the system.

The purpose of this investigation is to demonstrate a new method of correction signal damping of direct-drive stable platforms that provides effective damping, introduces no interferences into the system due to base motion, allows the system to track to its maximum capability, and requires only electrical connection to the stable platform.

The basic principle of this method of damping is to differentiate the correction signal from the gyroscope in a high-speed, closed-loop servomechanism, apart from the stable element, and introduce the differentiated signal as a damping signal into the stable platform servo drive. The idea is credited to Lees.

This method of damping is tested in theory and then employed in damping and existing direct-drive stable platform.

CHAPTER 2

PRESENTATION OF THE THEORY

There are many methods of damping servomechanisms in common use. Some of these methods use the output and its first or second time derivative in a feedback loop. Others modify the correction signal or the feedback signal. However, in the damping of stable platforms, none of these methods achieve optimum results. To illustrate this fact some of the operating principles of stable platforms are discussed.*

In the construction of a single-axis stable platform an integrating gyro unit is mounted on the stable platform such that the input axis is aligned with the axis of rotation of the controlled member. If the servo drive system, which drives the controlled member in response to the correction signal from the gyro, tracks perfectly, the controlled member is effectively locked to the inertial space reference of the gyroscope. Fig. 2-1 is a functional diagram of such a system. Stable platforms are required to track with high precision, to be small and light, and to remain independent of the motion of the vehicle in which they are carried over a period of time.

For high precision it is desirable to eliminate the gear train with its uncertainties from the servo drive system. (1)**

---

* Ref. 1 and 2 discuss stable platforms in detail.

** Numbers in parenthesis refer to numbered references in the bibliography.

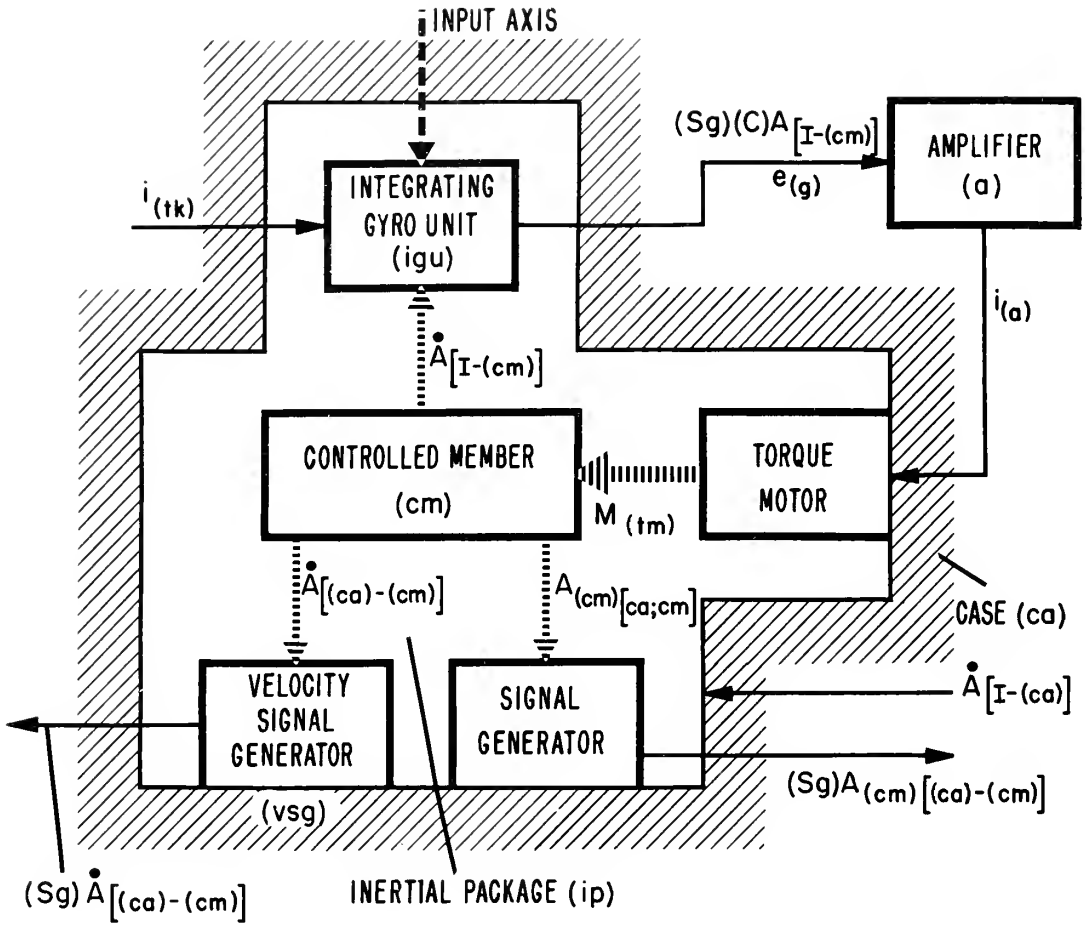

$i_{(tk)}$	=	input current to gyro torque generator
$e_{(g)} = (Sg)(C)A_{[I-(cm)]}$	=	gyro output voltage = correction signal
$i_{(a)}$	=	amplifier output current
$M_{(tm)}$	=	torque motor output torque
$\dot{A}_{[I-(cm)]}$	=	angular velocity of control member relative to an inertial space orientation for which the gyro unit voltage output has its null level
$\dot{A}_{[(ca)-(cm)]}$	=	angular velocity of the control member relative to the case
$A_{[(ca)-(cm)]}$	=	angle of control member relative to the case
$\dot{A}_{[I-(ca)]}$	=	angular velocity of the case relative to an inertial space orientation for which the gyro output voltage has its null level
IA	=	input axis of the stable element, i.e., the (igu)

Fig. 2-1 A direct-drive single-axis stable platform

Furthermore, the motor damping torque and torque due to viscous friction in the bearings and slip rings,

$$M_{(d)} = (-S_{(tm)}\left[\dot{A};M\right] + C_{(cm)(sp)})(\dot{A}\left[I-(cm)\right]-\dot{A}\left[I-(ca)\right])$$

is multiplied by the gear train ratio squared when transmitted through a gear train to the controlled member. The first term of this expression provides useful damping for the system; the other term is an interference to the system due to base motion. The error due to this interference has been greatly enlarged by the use of a gear train. It is, therefore, advantageous to employ a direct-drive servo system.[1]

The performance equation for a direct drive stable platform is derived in Equation Summary (1)*. From equation (3) it is evident that there is no inherent damping in a direct-drive system, if the small contribution of the motor damping torque and viscous friction are neglected.

The measurable outputs of the stable platform which may be used in a damping system are, the angle of the controlled member with respect to the case, $A\left[(ca)-(cm)\right]$, the angular velocity of the controlled member with respect to the case $\dot{A}\left[(ca)-(cm)\right]$ and the correct signal voltage, (Sg) (c) $A\left[I-(cm)\right]$.

Tachometer damping is frequently used to damp stable platforms. The performance equation for a stable platform with tachometer damping appears in Equation Summary 2, equation (4). Fig. A-3 shows a typical tachometer damping system.

The tachometer, attached to the controlled member directly, or through a gear train, generates a voltage proportional to the angular velocity of the controlled member with respect to the case, $\dot{A}\left[(ca)-(cm)\right]$. This voltage is fed back through the system to provide a damping torque on the controlled member.

The important feature of this damping method is that,

---

*Equations appear in Appendix A.

although damping is achieved, an interference input proportional to the angular velocity of the case with respect to inertial space, $S_{(sp)}\left[\dot{A};M\right]\ p\ A\left[I-(ca)\right]$, is introduced into the system.

If the system is a direct-drive stable platform, the sensitivity of the tachometer must be high to achieve adequate damping. If the stable platform is carried in a high-speed maneuvering craft, $\dot{A}\left[I-(ca)\right]$ may be large.

The interference torque introduced into the system by use of tachometer damping may be very large. In addition, the tachometer must be attached physically to the controlled member within the inertial package.

The advantages of tachometer damping are that such a system is relatively easy and cheap to construct and that the damping ratio is easily controlled by adjusting the tachometer sensitivity.

Another method of damping commonly used to damp stable platforms is lead modifier damping[4]. The performance equation for a stable platform with lead modifier damping appears in Equation Summary 3, equation (3). Fig. A-5 shows a lead modifier damped stable platform.

A lead modifier circuit such as described in Fig. A-4 is inserted in the forward path of the system. The effect of the lead modifier on the system may be discussed in view of its low, intermediate, and high frequency characteristics[4].

At low frequency the performance equation may be approximated by equation (7), Equation Summary 3.

The residual damping appearing in the equations arise principally from the motor damping torque and viscous friction which, in the absence of a gear train, are very small.

The damping ratio achieved at low frequency is the residual damping ratio multiplied by the characteristic time ratio, ν_{ld} ν_{ld} is generally determined by the damping ratio desired at

intermediate frequencies. A $\nu_{ld} = 10$ will provide approximately, $\zeta_{(ps)} = .7$, at intermediate frequency but only light damping at low frequency. The low frequency stiffness has been attenuated by the same factor, ν_{ld} Typical step function responses for a lead modifier damped positional servomechanism with high frequency stiffness held constant are shown in Fig. 2-2.

At intermediate frequencies the system can be made to operate like a well-damped, second-order system. Equation (8), Equation Summary 3.

At high forcing frequency equation (9) shows that only residual damping is present.

The system will be very lightly damped at low and high forcing frequency.

In a high gain system at low frequency, the amplitude of the response leads to saturation of the torque-motor windings and resultant unstable operation. At low frequency use of lead modifier damping requires either higher loop gain or results in a larger error at low frequency. A lag circuit may be added in order to increase the low-frequency stiffness. However, if the low-frequency stiffness is held constant, a loss of stiffness at high frequency makes the system sensitive to sudden changes in interference torques. No damping is provided by the addition of the lag network.

Use of the lead modifier in an a.c. loop will necessitate the insertion of a demodulator - remodulator section to provide a d.c. path for the lead network. A smoothing network must be added to suppress high frequency noise, passed by the lead modifier, causing saturation of the drive amplifier.

Lees proposed a new method of correction signal damping that has none of the disadvantages of conventional damping schemes when applied to a stable platform.

In this new method, the correction signal voltage from the

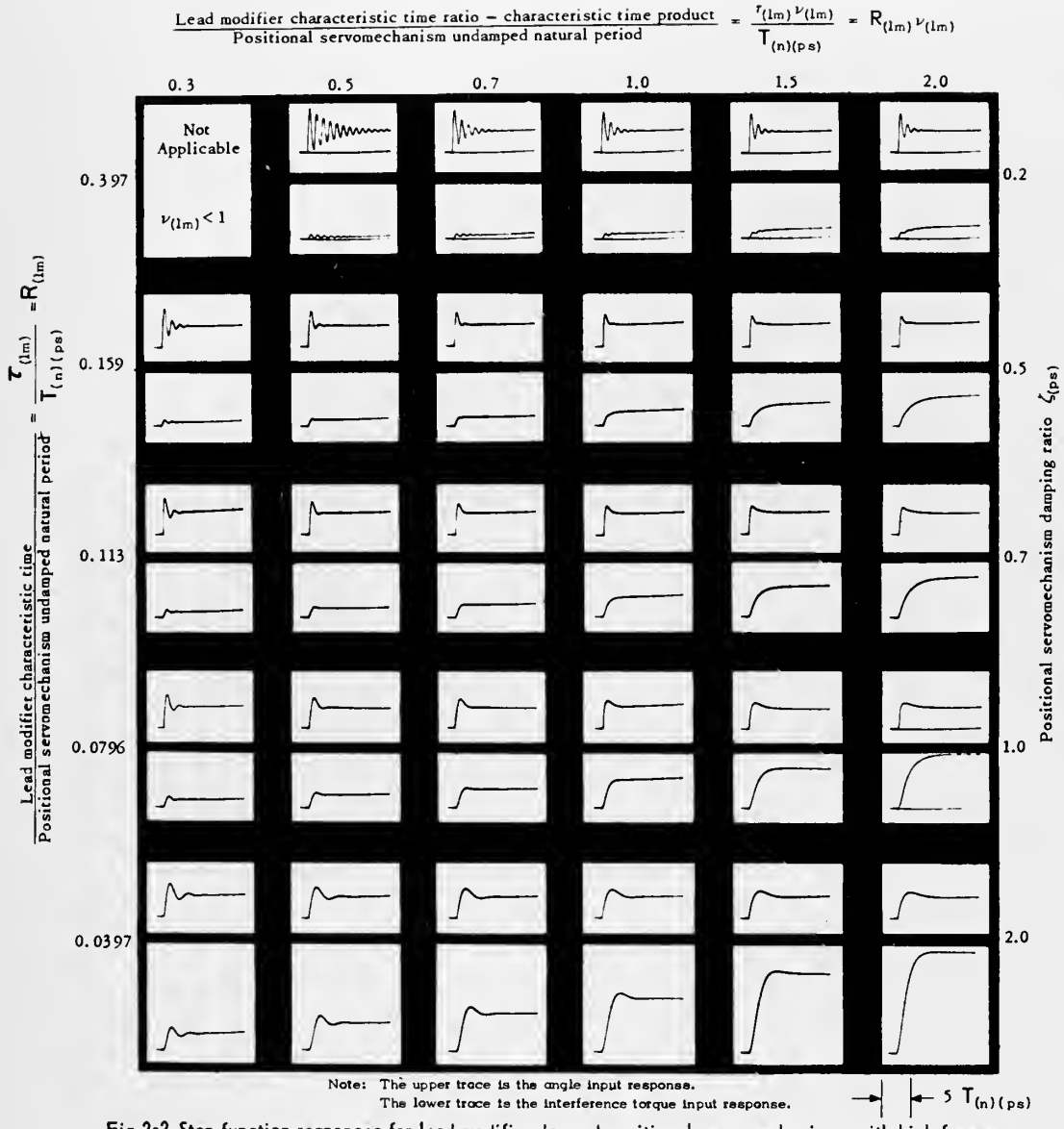

Fig.2-2 Step function responses for lead modifier damped positional servomechanisms with high-frequency stiffness held constant.

gyro is differentiated in a small, high-speed, direct-drive servo-mechanism and then sent back to the stable platform servo-drive system as a velocity damping signal.

Derivation Summary 1 is a development of the performance equations for a direct-drive, single-axis, stable-platform damped with a second-order servomechanism as shown functionally in Fig. A-6. Equations (12) and (13) are two forms of the final equations with $i_{(tk)} = 0$. Equation (19) shows the input to the system if $i_{(tk)}$ is not zero. Equation (11) shows the nature of the damping torque on the controlled member of the stable platform.

No terms appear in the equations that are proportional to the angular motion of the case with respect to inertial space, $\dot{A}\left[\bar{I} - (ca)\right]$, as a result of the damping signal so the system is truly space damped. The magnitude of the damping torque is easily controlled by adjusting the sensitivity of the damper-tachometer-amplifier. Another obvious feature is that the damping system requires only electrical connection with the main servo-drive.

The system is more easily discussed when viewed in parametric form as in equation (18) of Derivation Summary 1(c). Equation (18) is reduced to its characteristic form.

$$\left({}'p^2 + \frac{2\zeta_{(sp)}\ {}'p}{\left[\dfrac{{}'p^2}{\beta^2_{(ds)}} + \dfrac{2\,\zeta_{(ds)}\,{}'p}{\beta_{(ds)}} + 1\right]} + 1 \right)$$

The parameters that will cause a departure from standard second-order behavior of the system are the damping servo undamped natural frequency - stable platform undamped natural frequency ratio, ($\beta_{(ds)}$), stable platform damping ratio ($\zeta_{(sp)}$), and the damping servo damping ratio, ($\zeta_{(ds)}$).

The damping signal, $e_{(dta)}$ (See equation (9)), should ideally be proportional to the time-rate-of-change of the correction signal voltage, $(S_g)(C)\,A\left[\bar{I} - (cm)\right]$, in magnitude, and lead the

correction signal voltage in phase by 90 degrees. Any non-linearities or phase lags in the damping servo will cause a departure from the ideal situation. The stable platform behavior will be influenced by this departure from the ideal in direct proportion to the magnitude of the damping signal, that is to say, the magnitude of the damping ratio, $\zeta_{(sp)}$, called for. If the phase of the damping signal is correct, or nearly so, the non-linearity of the differentiation will only cause a variation of the damping ratio, $\zeta_{(sp)}$. A marked lag in the phase of the damping signal from the ideal will, however, introduce a forcing signal into the system leading to instability.

The obvious way to insure that the damping signal is of good quality is to set $\beta_{(ds)}$ so high that no appreciable lag in the damping servo can be detected at forcing frequencies for which the stable platform response is elastic. Even if the damping servo response is oscillatory, the stable platform will not respond to the high frequency oscillations.

It was estimated that good damping of the stable platform through a wide range of damping ratios, $\zeta_{(sp)}$, could be obtained with a combination of $\beta_{(ds)} = 10$ and any value of damping ratio for the damping servo, $\zeta_{(ds)}$, for which the damping servo was stable up to, and including $\zeta_{(ds)} = 1.0$. This can be seen graphically in Fig. 2-3 and 2-4 if the second-order responses shown are viewed as deviations of the damping signal from the ideal.

For a given $\beta_{(ds)}$ it is seen from Fig. 2-3 and 2-4 that an increase in the damping ratio of the damping servo, $\zeta_{(ds)}$, will result in increased phase deviation of the damping signal, $e_{(dta)}$, from the ideal. It would seem at first glance that the best signal could be obtained by setting, $\zeta_{(ds)}$, very low. The only bar to this proceedure is that oscillations of the damping servo although filtered by the stable platform torque motor may tend to saturate the power drive amplifier at high stable platform damping ratios, $\zeta_{(sp)}$

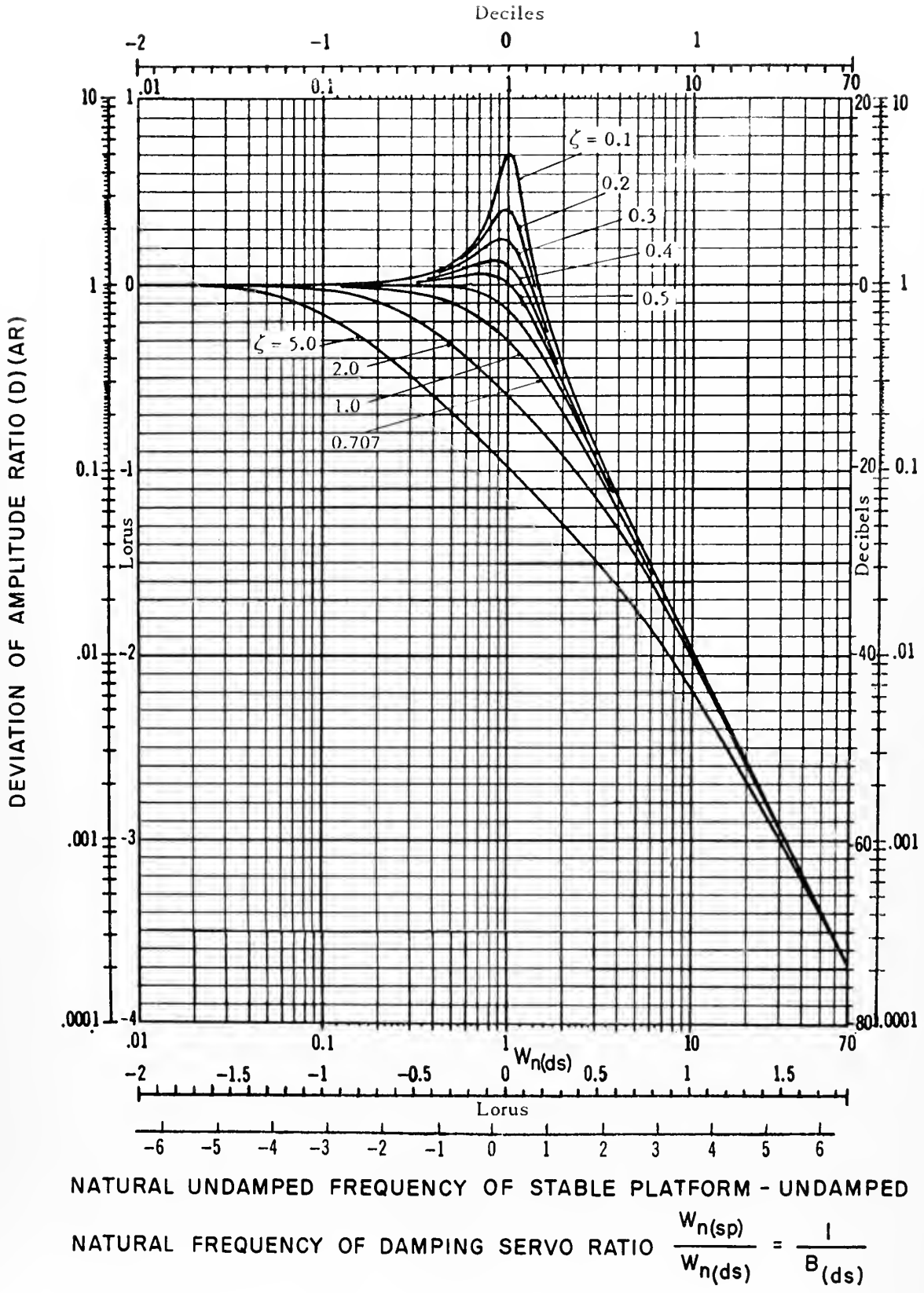

Fig. 2-3 Representing the deviation of $e_{(dta)}$ from the ideal at any particular value of $\beta_{(ds)}$

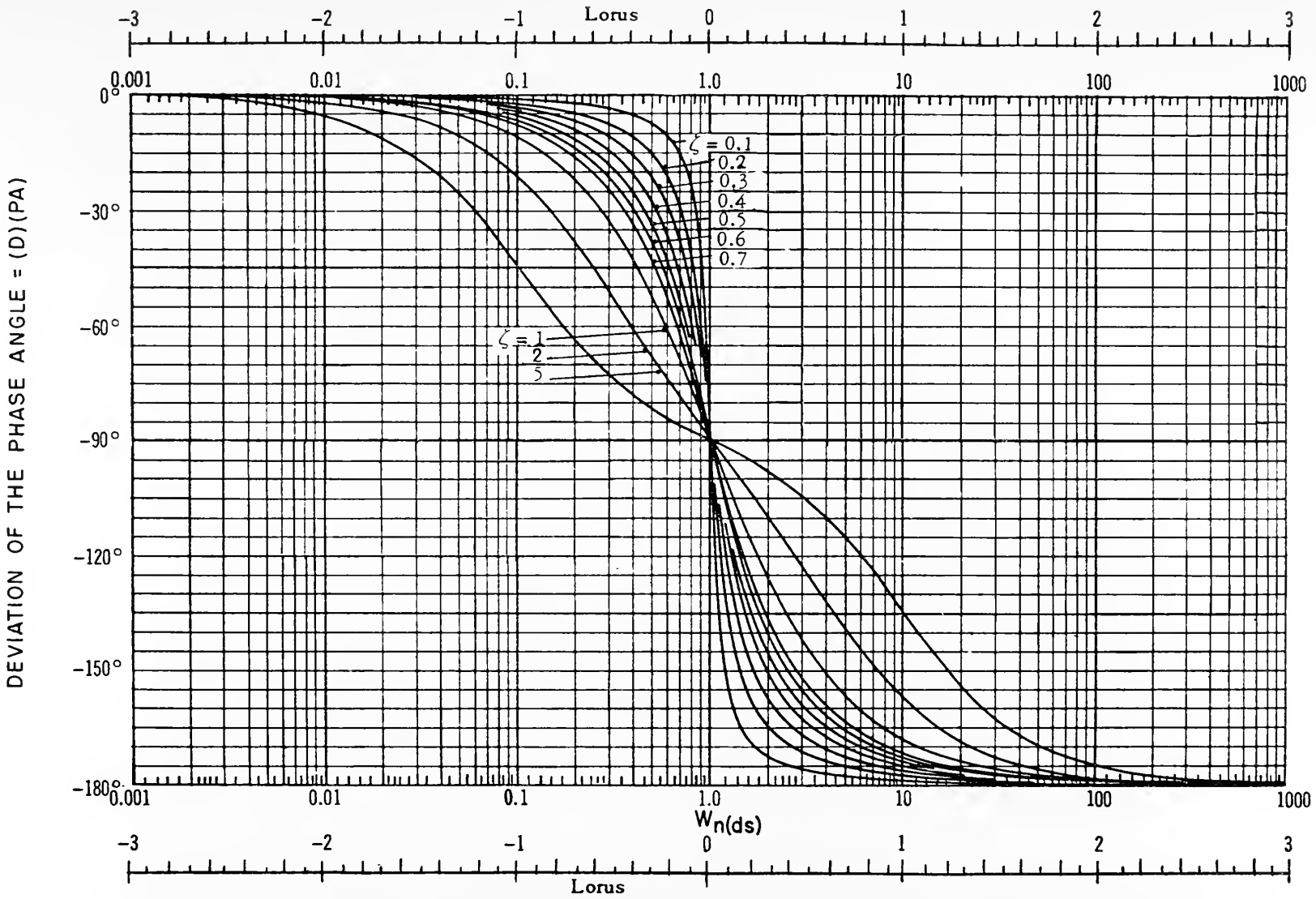

UNDAMPED NATURAL FREQUENCY OF STABLE PLATFORM - UNDAMPED NATURAL FREQUENCY OF THE DAMPING SERVO RATIO $\frac{W_{n(sp)}}{W_{n(ds)}} = \frac{1}{B_{(ds)}}$

Fig. 2-4 Representing the deviation of $e_{(dta)}$ from the ideal at any particular value of $\beta_{(ds)}$

The expected performance is now summarized. If the second-order approximation of the stable platform is valid, the system should behave as a well-damped second-order system for $\beta_{(ds)} \geq 10$ and for a wide range of damping ratios of the stable platform, $\zeta_{(sp)}$ and for the damping servo, $\zeta_{(ds)}$. For $\beta_{(ds)} < 10$ the system should behave properly at low damping ratios of the stable platform and over a wide range of damping ratios for the damping servo, but show oscillatory transient responses for combinations of high damping ratio for the stable platform and low damping ratio for the damping servo. It is expected that best overall performance will occur when the damping servo transient response is non-oscillatory ($\zeta_{(ds)} \cong .7$), $\beta_{(ds)} \geq 10$, and the damping ratio of the stable platform is set at approximately ($\zeta_{(sp)} \cong .7$).

Another feature of this particular damping system that is rather striking is pointed up by the performance equations. From equation (16) of Derivation Summary 1 (c), $\zeta_{(sp)}$ is proportional to the undamped natural frequency ($\omega_{n_{(sp)}}$) of the stable platform. Provided a $\beta_{(ds)} \geq 10$ is attainable, a particular damping servo unit may be used on many different systems, the low frequency systems requiring the highest damper-tachometer-amplifier gain for a specified damping ratio.

One feature that may or may not be desirable is shown in equation (19) of Derivation Summary 1 (c). The equation shows that the system adds a signal proportional to the time derivative of the input to the system. This will result in very rapid response but may also cause some oscillation in the system. This derivative input has the second order lag of the damping servo associated with it, and so there may be some combinations of $\beta_{(ds)}$, $\zeta_{(sp)}$, and $\zeta_{(ds)}$ that will give extremely rapid responses without oscillation. If oscillations in the transient response occur due to the derivative input, they would be expected at low damping ratios for the damping servo, $\zeta_{(ds)}$, and high damping ratio for the stable platform, $\zeta_{(sp)}$.

CHAPTER 3

ANALOG COMPUTER ANALYSIS OF BASIC THEORY

Analysis of the performance equations of Derivation Summary 1 indicates that the performance of a direct-drive, single-axis stable platform can be approximated by the performance of a second-order positional servomechanism.

In order to test the damping theory outlined in Chapter 2, the performance equation of a second-order positional servomechanism, damped by another second-order positional servomechanism was set up on an analog computer. The performance equation of the resulting system appears as equation (4) of Equation Summary (4). Fig. A-7 shows the analog computers set up.

A survey of the transient response of the system was made using a step function as the input. The variables for this survey were the damping ratio of the main servo loop, $\zeta_{(ps)}$; the damping ratio of the damping servo loop, $\zeta_{(ds)}$; and the ratio of the undamped-natural-frequency of the damping servo loop to the undamped-natural-frequency of the main servo loop, $\beta_{(ds)}$. The output was displayed on an oscillograph and photographed.

The results of the survey appear in Fig. 5-1, 5-3, 5-5, 5-7, 5-9.

The analog computer solutions indicated that the proposed method of damping could be used to damp an actual stable platform.

CHAPTER 4

THE STABLE PLATFORM AND TESTING PROCEDURE

A high-speed, second-order, closed-loop servomechanism was assembled and installed to damp a single-axis, direct-drive, stable platform in being at the Instrumentation Laboratory of Massachusetts Institute of Technology. See Fig.A-8. The stable platform was designed to test the 20IG, 10^4, integrating gyros developed at that facility. A description of the components of the system appears in Appendix B.

The original design incorporated a lead modifier network for damping in the forward loop. This system had all of the characteristics ascribed to lead modifier damping. The tracking precision required, made it necessary to set the stiffness so high that saturation of the torque-motor windings occurred outside an extremely narrow notch.

A small step torque on the controlled member would cause oscillations of table, saturating the torque motor windings and causing unstable operation.

Attempts were made to obtain transient response and frequency response data for comparison with responses using the damping servomechanism. However, this effort was abandoned because no stable responses could be obtained.

Due to the high static stiffness requirement of the system. the lead modifier characteristic time ratio was limited to 4.5, which is not optimum for lead modifier damping.

The only change made to the system before installing the damping servomechanism was the removal of the lead modifier

network.

The damping servomechanism was manufactured from parts available at the laboratory. A Fisher, 50 watt amplifier with matching preamplifier; a Kearfott R 800 IA-A, motor generator, an ultra low torque potentiometer, and a demodulator-amplifier made up the major components of the system.

The stiffness of the stable platform was set to given an undamped natural frequency, $\omega_{n_{(sp)}} = 10$ rad/sec. The value was measured by recording the transient response of the system at a low damping ratio. The $\omega_{n_{(sp)}}$ was intentionally set lower than normal in order to obtain the same range of frequency ratio, $\beta_{(ds)}$ that were used in the analog computer survey.

In order to obtain the transient response of the system, the gyro was torqued by a current to the torque generator to cancel the effect of earth rate and gyro drift. The gyro measuring reference was thus shifted from inertial space to an earth reference. The step function input was generated by displacing the platform manually, and suddenly releasing it. The angular position of the platform with respect to case about the input axis of the gyro was recorded as the output of the system.

The gain control on the damping servo amplifier was calibrated to read $\omega_{n_{(ds)}}$. This was done by recording the step response of the damping servo at a low damping ratio. The damping ratio of the damping servo, $\zeta_{(ds)}$ was determined from step responses for various settings of the tachometer-potentiometer, and the dial calibrated. The gain control of the demodulator-amplifier was calibrated for damping ratio of the stable platform, $\zeta_{(sp)}$ by observing the transient response of the stable platform at a $\beta_{(ds)} = 15$. From the computer results it was considered that $\beta_{(ds)} = 15$ was well above the $\beta_{(ds)}$ required for satisfactory damping.

The transient response of the system was recorded on a

Sanborn Recorder as the output voltage of the microsyn signal generator on the controlled member of the stable platform.

The transient responses appear in Fig. 5-2, 5-4, 5-6, 5-8, 5-10.

Although it was impossible to record data to be presented in this report due to the limited angular range of the signal generator on the controlled member, large torques were applied to the table by means of a signal to the gyro torque generator causing rotation of the table. Repeated, rapid reversals of the signal direction, at the highest rate obtainable, approximately five radians per second, were made and the table remained positively damped.

CHAPTER 5

COMPARISON OF THE ANALOG COMPUTER SOLUTIONS AND THE RESPONSES OF THE STABLE PLATFORM

A comparison of the transient responses for the analog computer solution and the actual stable platform with damping servomechanism shows good correlation for all values of the damping ratio of the stable platform, $\zeta_{(sp)}$. The transient responses appear in Figs. 5-1 to 5-10.

From the Tables 5-1 and 5-2 a comparison of the predicted and actual values for percent overshoot indicate that the actual stable platform had three or four times the overshoot of the computer system for $\zeta_{(sp)} = .5$ and $\zeta_{(sp)} = .7$. However, at $\zeta_{(sp)} = 1.0$ and $\zeta_{(sp)} = 2.0$ there is much better agreement. It is believed that the discrepancy in per cent overshoot at the lower values of $\zeta_{(sp)}$ was due to the fact that the damping was not set high enough to produce the characteristic transient response for these damping ratios. It is evident from the responses at successively higher damping ratios, $\zeta_{(sp)}$ that the overshoot can be set to any desired value by changing $\zeta_{(sp)}$.

A comparison of response times show good agreement for the lower values of $\zeta_{(sp)}$ However, at higher values of $\zeta_{(sp)}$ the predicted response times are longer than the actual response times. This apparent discrepancy can be explained by the fact that it was difficult to determine the point of tangency of the rise of the response to the final steady-state value from the oscillograph pictures.

Comparison of the overshoot-undershoot ratio for the predicted and actual responses show excellent agreement except in the fringe areas where the responses become more oscillatory

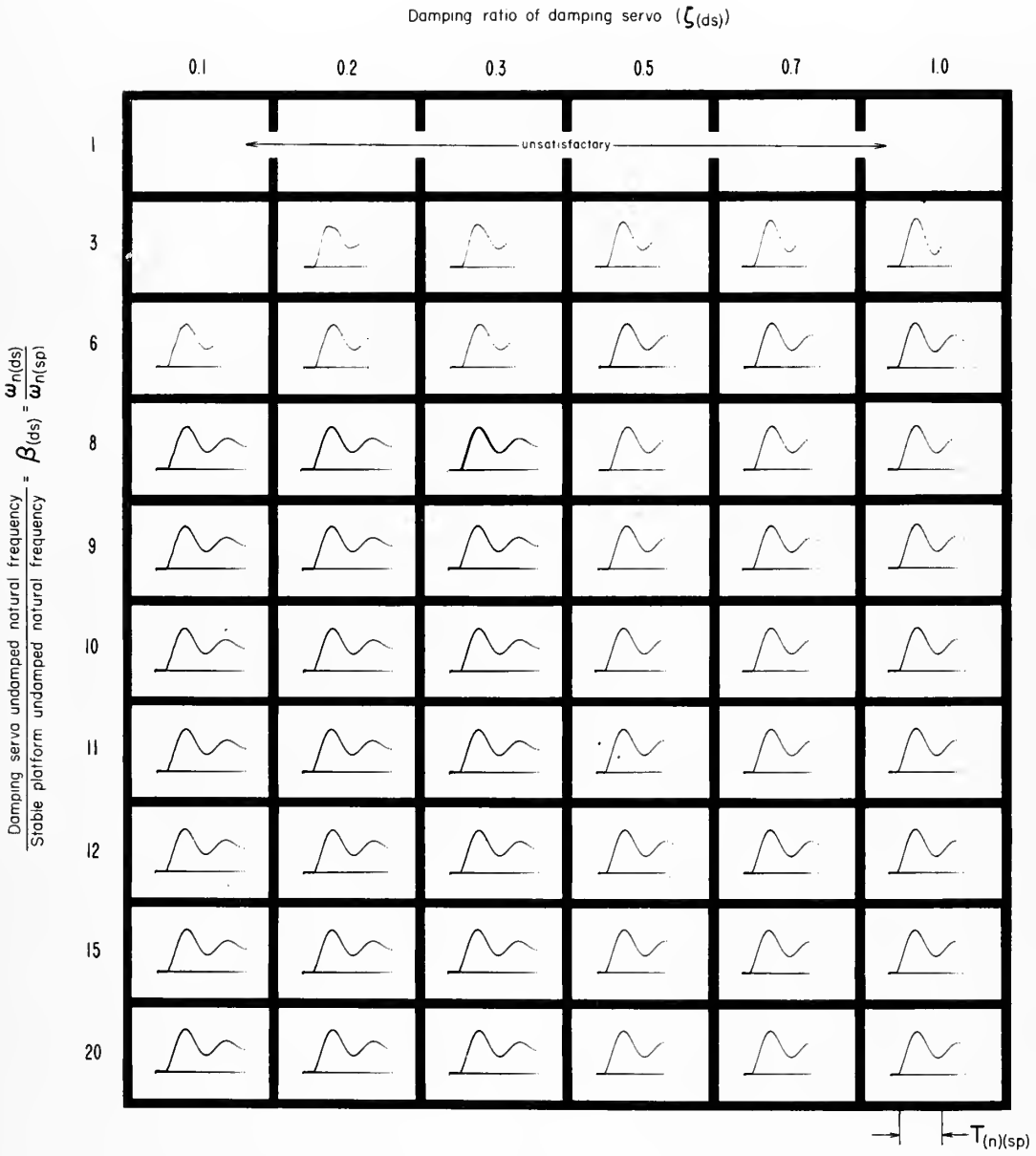

Fig. 5-1 Predicted transient response of stable platform with damping servomechanism for a damping ratio of the stable platform, $\zeta_{(sp)} = 0.2$

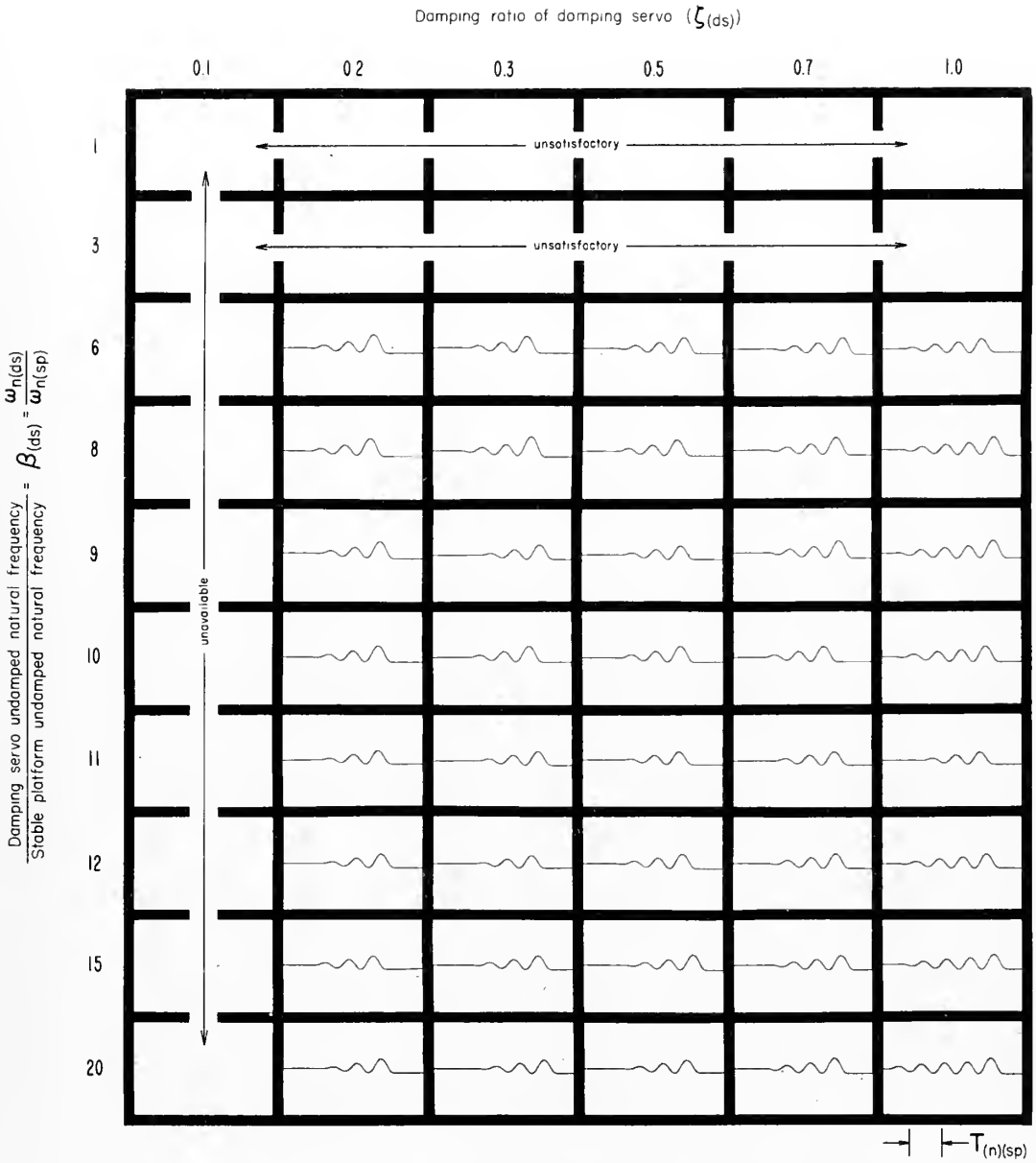

Fig. 5-2 Actual transient response of stable platform with damping servomechanism for a damping ratio of the stable platform, $\zeta_{(sp)} = 0.2$

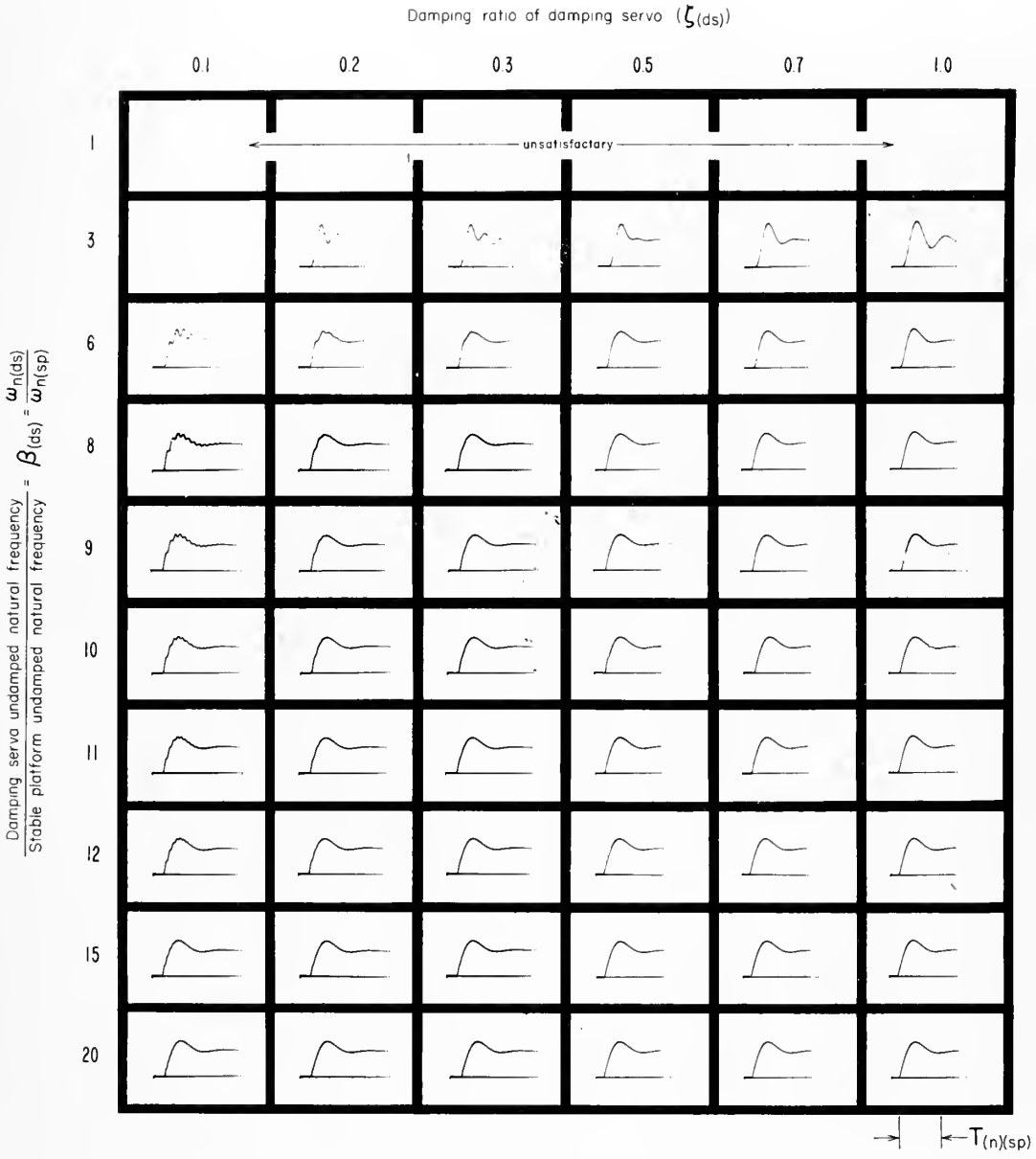

Fig 5-3 Predicted transient response of stable platform with damping servomechanism for a damping ratio of the stable platform, $\zeta_{(sp)} = 0.5$

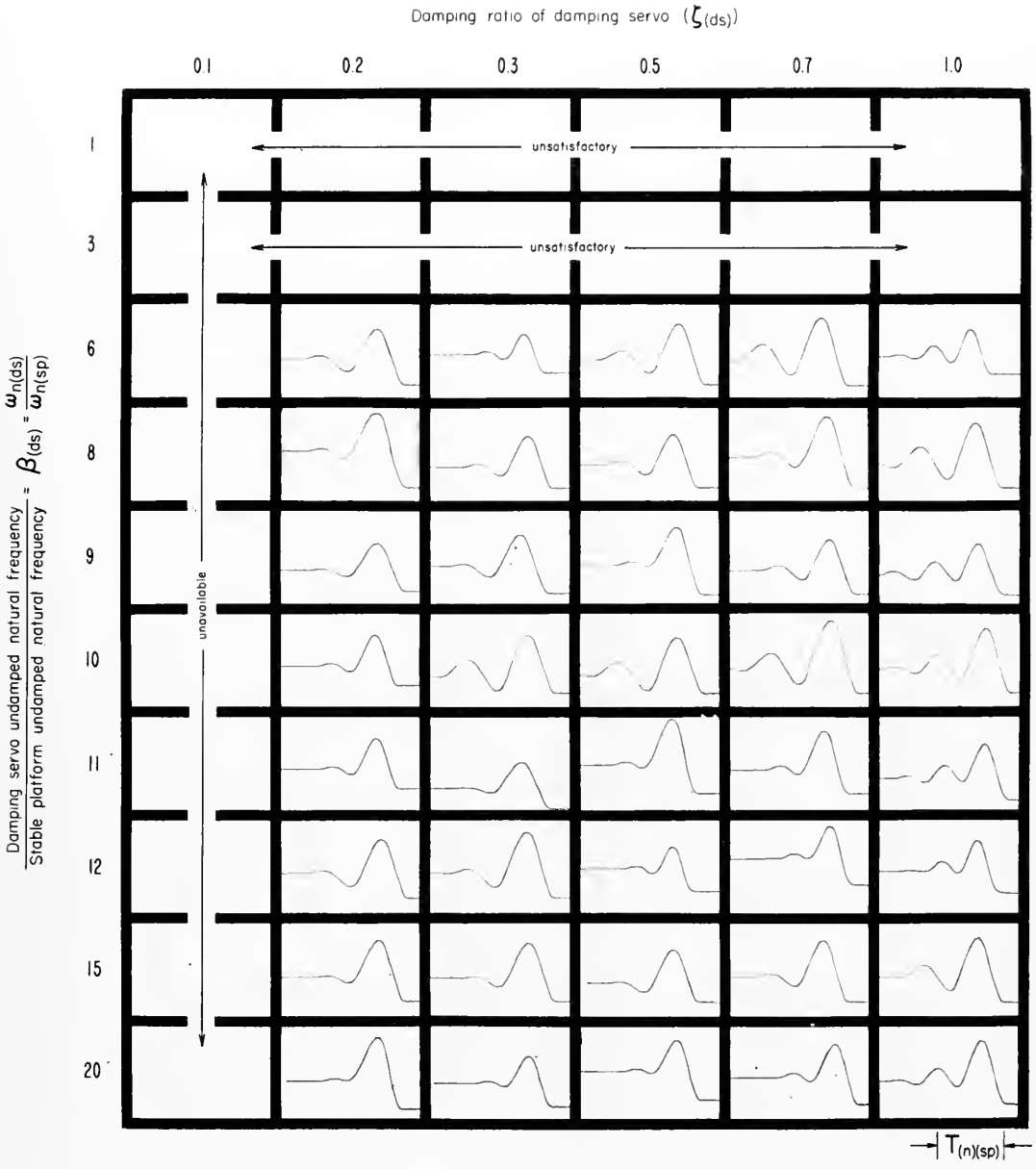

Fig. 5-4 Actual transient response of stable platform with damping servomechanism for a damping ratio of the stable platform, $\zeta_{(sp)} = 0.5$

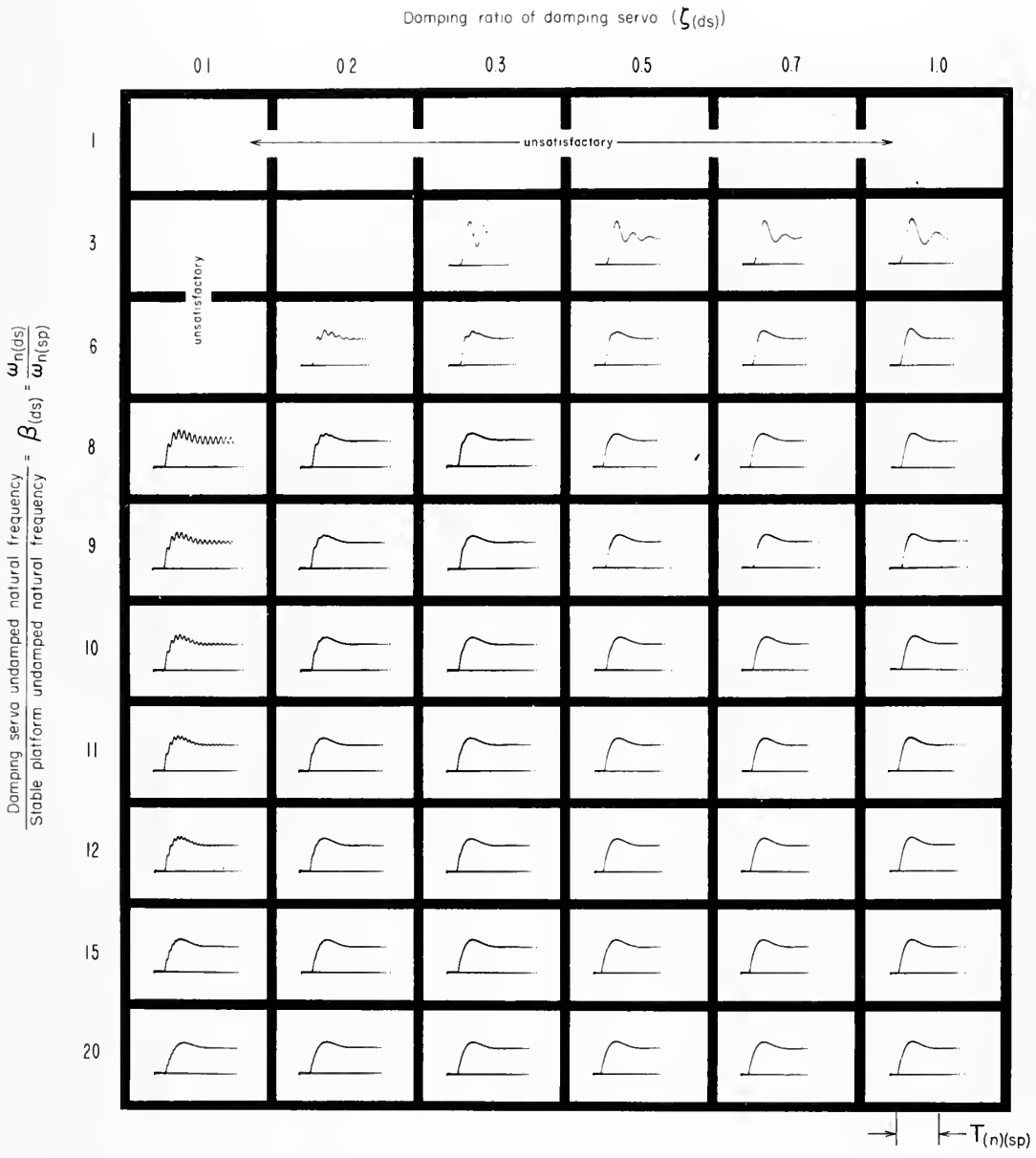

Fig 5-5 Predicted transient response of stable platform with damping servomechanism for a damping ratio of the stable platform, $\zeta_{(sp)} = 0.7$

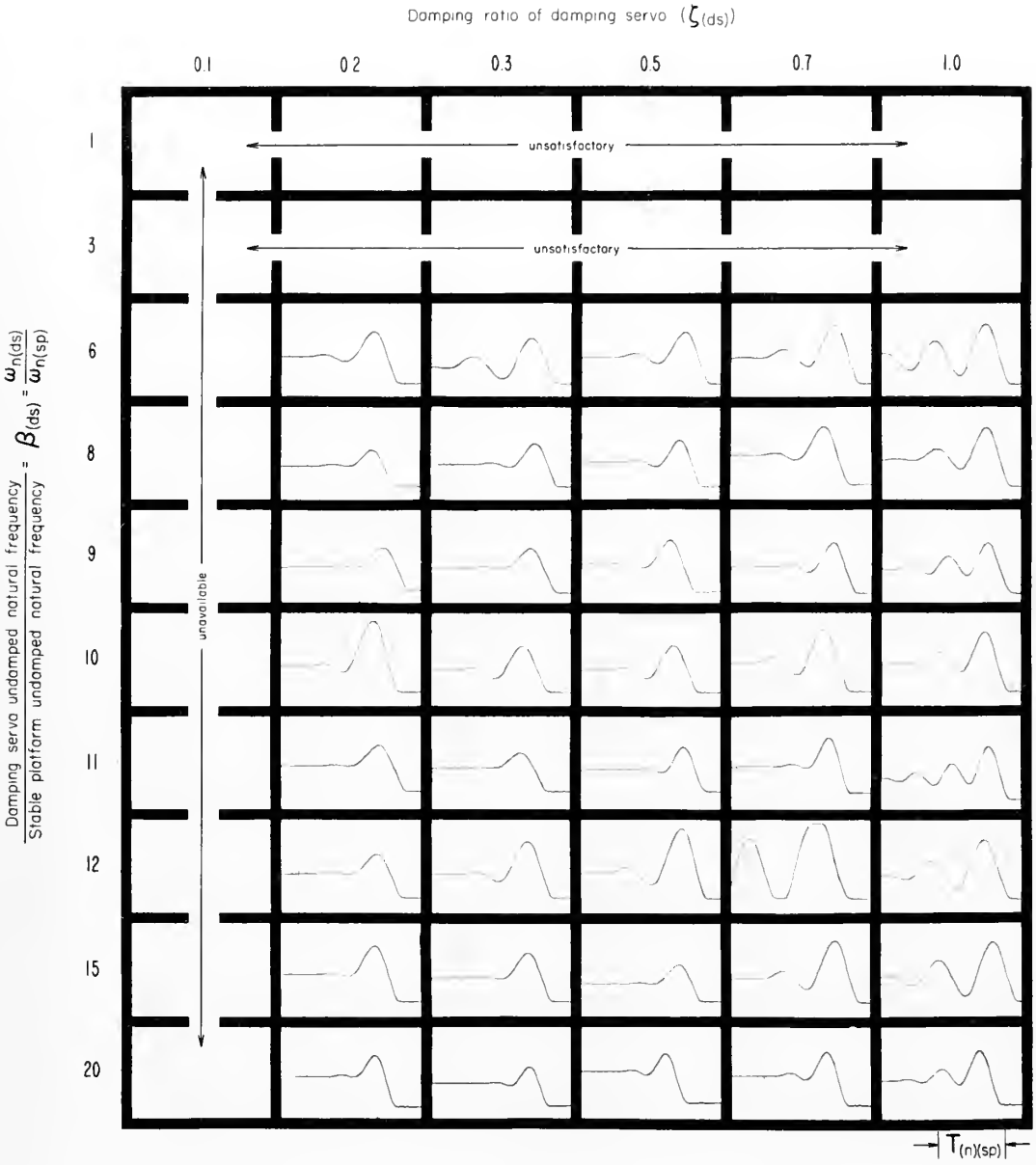

Fig. 5-6 Actual transient response of stable platform with damping servomechanism for a damping ratio of the stable platform, $\zeta_{(sp)} = 0.7$

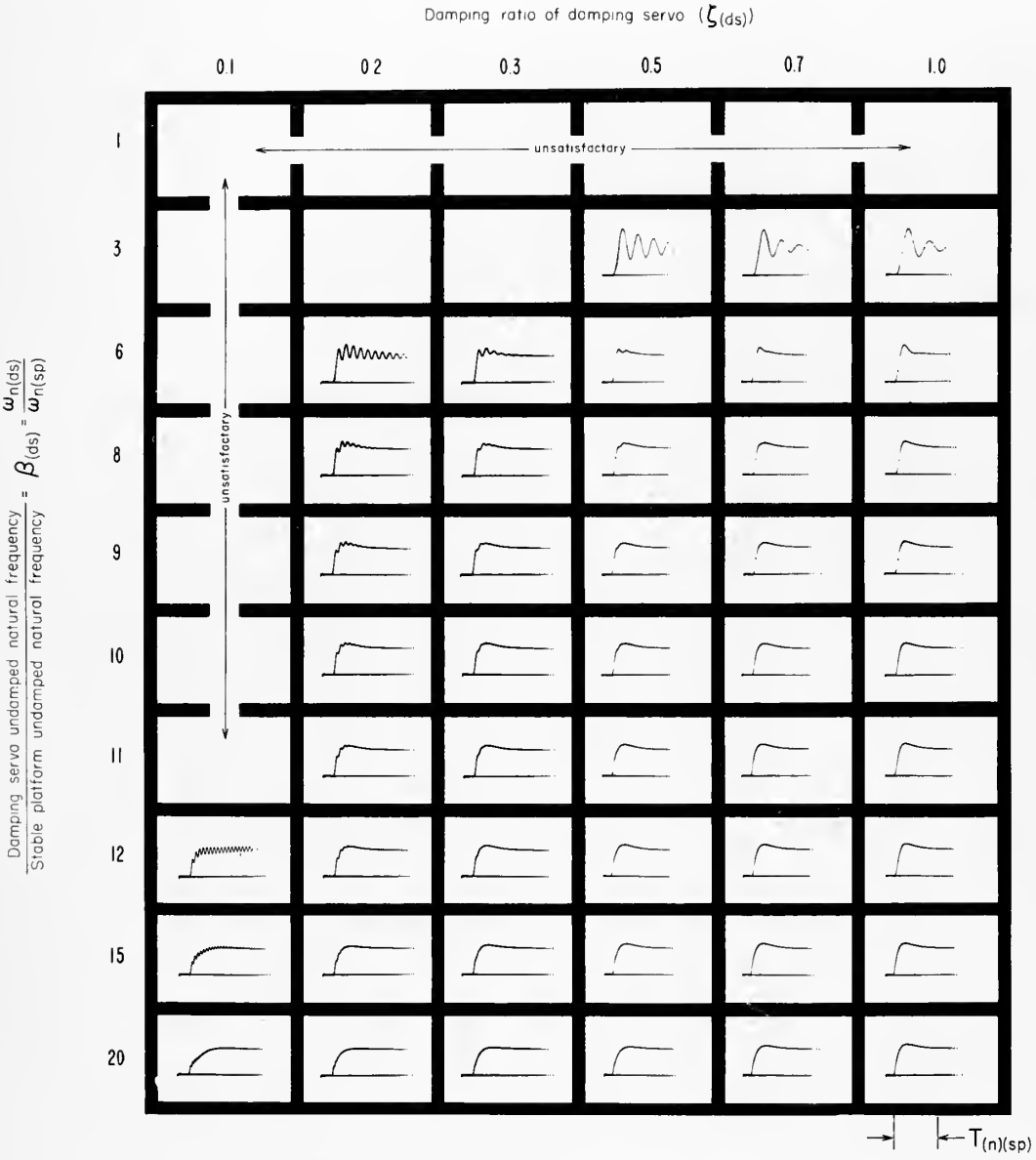

Fig 5-7 Predicted transient response of stable platform with damping servomechanism for a damping ratio of the stable platform, $\zeta_{(sp)} = 1.0$

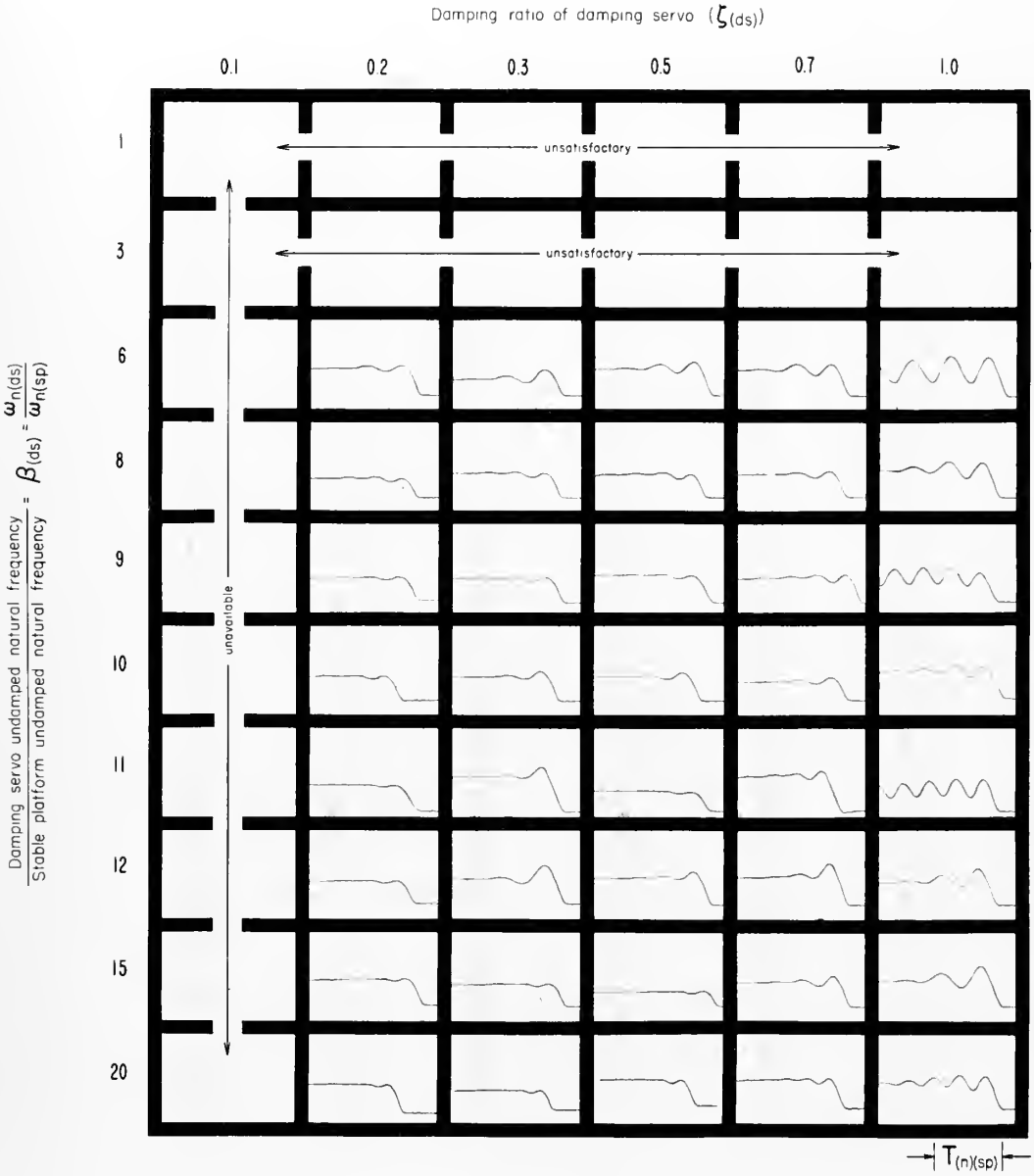

Fig. 5-8 Actual transient response of stable platform with damping servomechanism for a damping ratio of the stable platform, $\zeta_{(sp)} = 1.0$

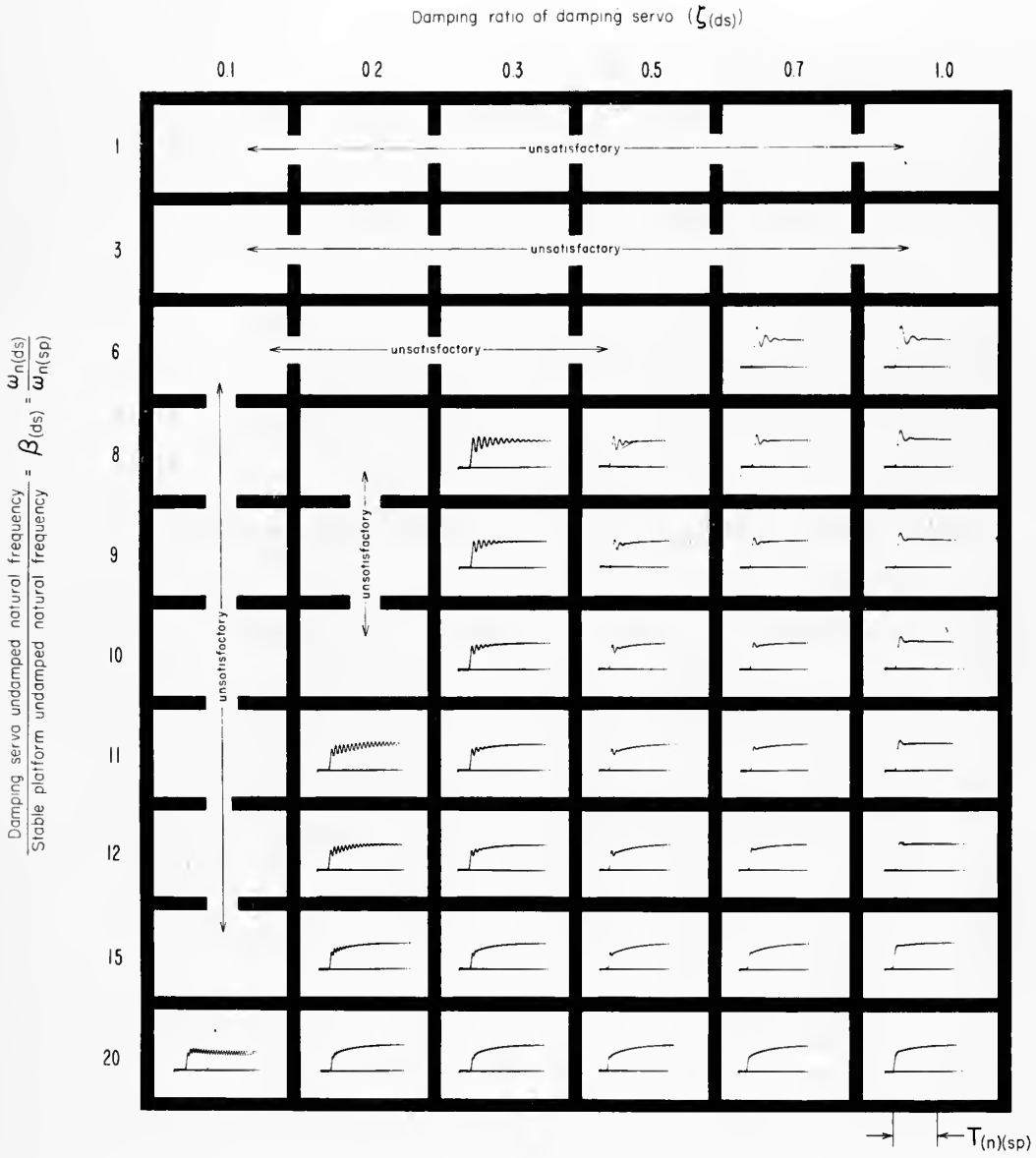

Fig. 5-9 Predicted transient response of stable platform with damping servomechanism for a damping ratio of the stable platform, $\zeta_{(sp)} = 2.0$

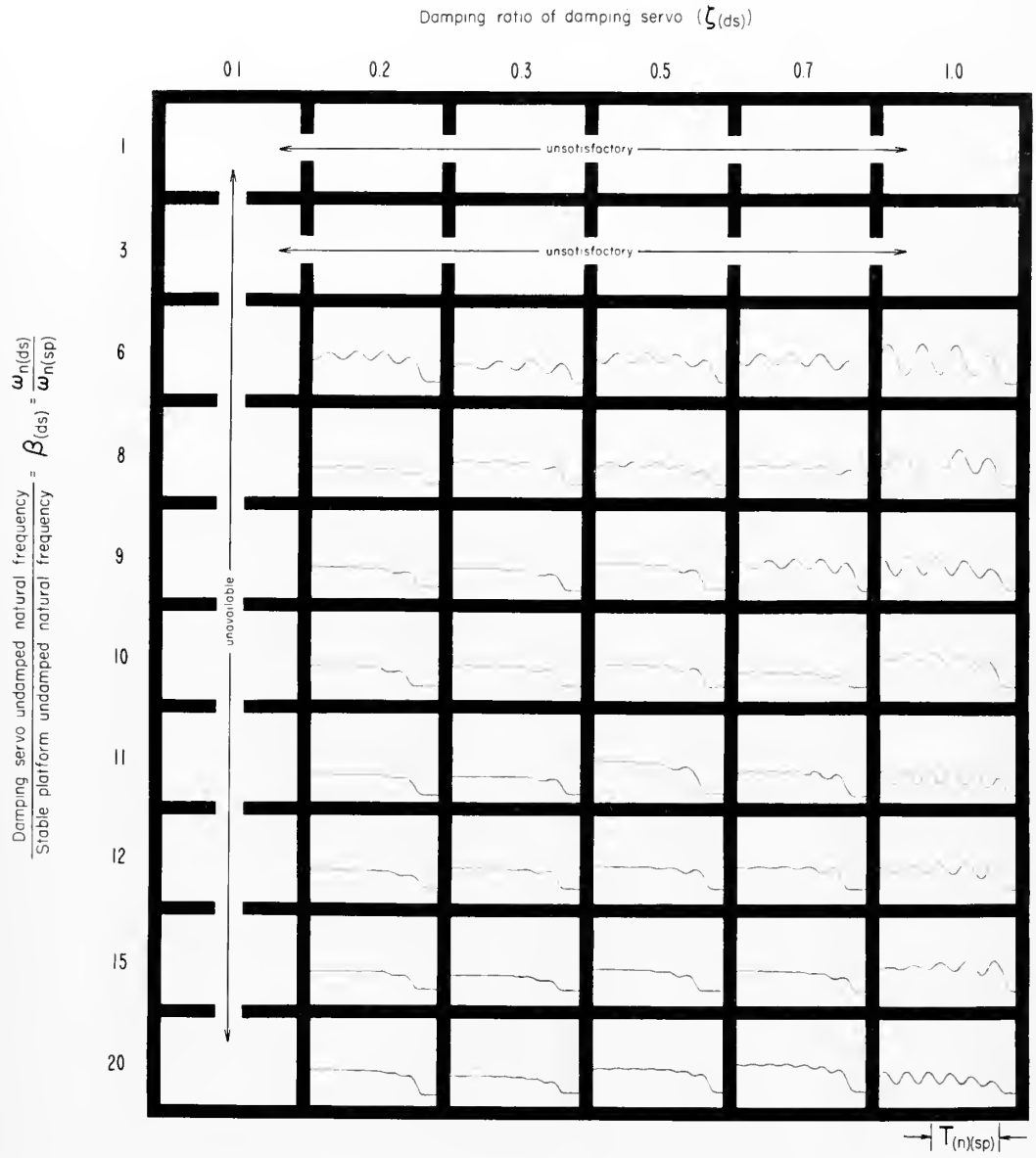

Fig 5-10 Actual transient response of stable platform with damping servomechanism for a damping ratio of the stable platform, $\zeta_{(sp)} = 2.0$

UNDAMPED NATURAL FREQUENCY OF DAMPING SERVOMECHANISM / UNDAMPED NATURAL FREQUENCY OF STABLE PLATFORM $= \beta_{(ds)} = \frac{W_{n(ds)}}{W_{n(sp)}}$

Damping Ratio of Stable Platform [$\zeta_{(sp)}$] = .5

	$\zeta_{(ds)}$ = .2		$\zeta_{(ds)}$ = .3		$\zeta_{(ds)}$ = .5		$\zeta_{(ds)}$ = .7		$\zeta_{(ds)}$ = .1	
	Pred.	Actual	Pred.	Actual	Pred.	Actual	Pred.	Actual	Pred.	Actual
1	◄				Unsatisfactory Response —					►
3	U	U	U	U	60 1.0 2/2	U	60 1.0 2/1	U	70 1.9 3/2	U
6	30 1.2 1/1	120 1.4 2/1	30 1.3 1/1	120 1.1 2/1	30 1.2 1/1	140 1.4 2/1	30 1.2 1/1	150 1.7 2/2	50 1.2 1/1	150 1.5 3/2
8	30 1.2 1/1	100 1.3 2/1	30 1.3 2/1	150 1.2 2/1	30 1.2 1/1	130 1.3 2/1	30 1.3 1/1	130 1.4 2/1	40 1.2 1/1	160 1.7 2/2
9	30 1.2 1/1	130 1.3 2/1	30 1.3 1/1	120 1.3 2/1	30 1.2 1/1	130 1.2 2/1	30 1.3 1/1	120 1.3 2/1	40 1.2 1/1	150 1.8 3/2
10	30 1.2 1/1	170 1.1 2/1	30 1.2 1/1	210 1.8 2/1	30 1.2 1/1	220 1.6 2/1	30 1.3 1/1	190 1.5 2/2	35 1.2 1/1	160 1.8 3/2
11	30 1.2 1/1	160 1.1 2/1	30 1.2 1/1	120 1.0 1/1	30 1.2 1/1	160 1.2 2/1	30 1.2 1/1	160 1.1 2/1	35 1.2 1/1	160 1.6 3/2
12	30 1.2 1/1	120 1.3 2/1	30 1.2 1/1	158 1.4 2/1	30 1.2 1/1	100 1.0 2/1	30 1.3 1/1	130 1.1 2/1	35 1.2 1/1	150 1.2 2/1
15	30 1.2 1/1	140 1.2 2/1	30 1.2 1/1	150 1.2 2/1	30 1.2 1/1	170 1.2 2/1	30 1.3 1/1	140 1.2 2/1	35 1.3 1/1	160 1.4 2/1
20	30 1.2 1/1	160 1.0 2/1	30 1.2 1/1	110 1.0 2/1	30 1.2 1/1	110 1.0 2/1	30 1.2 1/1	120 1.1 2/1	35 1.3 1/1	170 1.4 2/2

Table 1. Comparison between predicted and actual step function response for various values of $\beta_{(ds)}$, $\zeta_{(sp)}$, and $\zeta_{(ds)}$ for the correction signal damped stable platform. The values of actual response were taken from Sanborn recorder tape to the nearest 10% and predicted response was read from the original photographs of the analogue computer solution.

Damping Ratio of Stable Platform [$\zeta_{(sp)}$] = .7

$\zeta_{(ds)}$ = .2		$\zeta_{(ds)}$ = .3		$\zeta_{(ds)}$ = .5		$\zeta_{(ds)}$ = .7		$\zeta_{(ds)}$ = 1.0	
Pred.	Actual	Pred.	Actual	Pred.	Actual	Pred.	Actual	Pred.	Actual
			Unsatisfactory Response						
U	U	U	U	60 1.6 4/3	U	60 1.5 3/2	U	70 1.9 3/2	U
U	100 1.2 2/1	30 .85 1/0	140 1.5 2/1	20 .75 1/0	90 1.2 2/1	30 .75 1/0	140 1.3 2/1	40 .60 1/0	160 2.2 3/3
30 .90 1/0	70 1.0 2/1	20 .85 1/0	90 .90 1/1	20 .75 1/0	80 1.0 2/1	30 .75 1/0	100 1.2 2/1	30 .70 1/0	110 1.3 2/1
30 .90 1/0	80 1.0 2/1	25 .85 1/0	80 .90 1/1	25 .75 1/0	80 1.0 1/1	25 .75 1/0	100 1.1 2/1	30 .70 1/0	110 1.6 3/2
30 .90 1/0	160 1.2 2/1	25 .85 1/0	110 1.3 2/1	20 .75 1/0	120 1.2 1/1	28 .80 1/0	110 1.3 2/1	28 .75 1/0	110 1.5 3/2
25 .90 1/0	80 .75 1/0	25 .90 1/0	70 .65 1/0	25 .75 1/0	90 .75 1/1	30 .80 1/0	100 1.0 2/1	30 .75 1/0	160 1.9 4/3
25 .90 1/0	80 .65 1/1	25 .90 1/0	140 1.2 2/1	25 .75 1/0	170 1.3 2/1	30 .80 1/0	✓	30 .75 1/0	150 1.6 2/2
25 .90 1/0	100 .70 1/1	25 .90 1/0	100 .90 1/1	25 .75 1/0	90 .60 1/0	25 .80 1/0	140 1.3 2/1	25 .75 1/0	120 1.6 2/2
20 .90 1/0	70 .80 2/1	25 .90 1/0	70 .65 1/1	20 .80 1/0	60 .70 1/1	25 .80 1/0	110 1.0 2/1	20 .80 1/0	110 1.4 3/2

(cont'd)

Percent Overshoot

Response Time

$T_{(n)_{(sp)}}$

Number of Overshoots

Number of Undershoots

$$T_{(n)_{(so)}} = \frac{1}{f_{(n)_{(so)}}} = \frac{1}{1.5 \text{ cps}} \quad \text{for Actual Data}$$

Table I (cont'd.)

UNDAMPED NATURAL FREQUENCY OF DAMPING SERVOMECHANISM / UNDAMPED NATURAL FREQUENCY OF STABLE PLATFORM = $\beta_{(ds)} = \frac{\omega_{n(ds)}}{\omega_{n(sp)}}$

Damping Ratio of Stable Platform [$\zeta_{(sp)}$] = 1.0

	$\zeta_{(ds)}$ = .2		$\zeta_{(ds)}$ = .3		$\zeta_{(ds)}$ = .5		$\zeta_{(ds)}$ = .7		$\zeta_{(ds)}$ = 1.0	
	Pred.	Actual	Pred.	Actual	Pred.	Actual	Pred.	Actual	Pred.	Actual
1	Unsatisfactory Response									
3	Unsatisfactory Response									
6	U	10 .85 2/0	U	50 .90 2/0	20 .65 1/0	20 .85 2/0	25 .65 1/0	20 .75 1/0	30 .40 1/0	70 3.1 6/5
8	U	0 .65 0/0	10 .75 1/0	0 .60 0/0	15 .65 1/0	0 .60 0/0	10 .75 1/0	10 .70 2/0	20 .70 1/0	27 1.3 3/2
9	U	0 .55 0/0	10 .75 1/0	0 .75 2/0	10 .75 1/0	0 .60 0/0	15 .75 1/0	20 .90 3/0	20 .70 1/0	U
10	15 .75 1/0	0 .55 0/0	15 .70 1/0	20 .75 2/0	10 .75 1/0	15 .65 2/0	15 .70 1/0	15 .78 2/1	20 .70 1/0	25 1.3 3/0
11	10 .70 1/0	0 .55 0/0	10 .70 1/0	0 .55 0/0	10 .75 1/0	15 .85 2/0	15 .70 1/0	15 .84 2/0	20 .70 2/0	U
12	10 .65 1/0	0 .55 0/0	10 .70 1/0	50 .85 1/0	10 .75 1/0	20 .60 2/0	10 .70 1/0	50 .80 2/0	15 .70 1/0	60 1.1 2/1
15	5 .60 0/0	5 .50 0/0	10 .65 1/0	0 .54 0/0	10 .75 1/0	5 .50 1/0	10 .70 1/0	20 .80 2/0	15 .65 1/0	60 1.2 2/1
20	0 .40 0/0	0 .40 0/0	0 .35 0/0	0 .40 0/0	0 .35 0/0	0 .45 0/0	0 .65 1/0	5 .51 2/1	10 .65 1/0	30 1.4 4/3

Table II. Comparison between predicted and actual step function response for various values of $\beta_{(ds)}$, $\zeta_{(sp)}$, and $\zeta_{(ds)}$ for the correction signal damped stable platform. The values of actual response were taken from Sanborn recorder tape to the nearest 10% and predicted response was read from the original photographs of the analogue computer solution.

Damping Ratio of Stable Platform [$\zeta_{(sp)}$] = 2.0

$\zeta_{(ds)}$ = .2		$\zeta_{(ds)}$ = .3		$\zeta_{(ds)}$ = .5		$\zeta_{(ds)}$ = .7		$\zeta_{(ds)}$ = 1.0	
Pred.	Actual	Pred.	Actual	Pred.	Actual	Pred.	Actual	Pred.	Actual
			Unsatisfactory Response						
			Unsatisfactory Response						
U	U	U	U	U	U	50 .85 3/3	U	50 .70 3/2	U
U	U	U	U	20 .75 4/2	U	25 .60 2/1	U	30 .40 2/2	U
U	0 .55 0/0	0 1.1 0/0	0 .51 0/0	0 1.1 0/0	0 .94 0/0	0 .90 0/0	U	25 .30 1/1	U
U	0 .50 0/0	0 1.0 0/0	0 .54 0/0	0 1.2 0/0	0 .54 0/0	0 .90 0/0	U	20 .3 1/1	U
0 - 0/0	0 .51 0/0	0 1.6 0/0	0 .50 0/0	0 1.2 0/0	0 .60 0/0	0 .95 0/0	U	10 .35 1/0	U
0 - 0/0	0 .50 0/0	0 1.3 0/0	0 .40 0/0	0 1.2 0/0	0 .50 0/0	0 1.1 0/0	U	0 1.4 1/0	U
0 1.4 0/0	0 .43 0/0	0 1.4 0/0	0 .65 0/0	0 1.3 0/0	0 .65 0/0	0 1.2 0/0	U	0 1.5 0/0	U
0 1.4 0/0	0 .50 0/0	0 1.4 0/0	0 .52 0/0	0 1.5 0/0	0 .60 0/0	0 1.3 0/0	U	0 1.7 0/0	U

(cont'd)

Percent Overshoot

Response Time

$T_{(n)}$ = $\frac{1}{f_{(n)}}$ = $\frac{1}{1.5 \text{ cps}}$ for Actual Data
(sp) (sp)

$T_{(n)}$
(sp)

Number of Overshoots

Number of Undershoots

Table II (cont'd.)

and border on being unsatisfactory.

In some areas, particularly in the $\zeta_{(sp)} = 2.0$ region predicted responses, that were considered to be unsatisfactory, were included to demonstrate the two oscillatory modes of the system. At the same values of $\zeta_{(sp)}$, $\zeta_{(ds)}$, and $\beta_{(ds)}$ the higher mode is not present in the response of the actual system. It is believed that actual system in this overdamped condition is too sluggish to follow the small oscillations.

Evidence that the two operating modes do exist in the actual system can be seen by examining the responses at $\zeta_{(ds)} = .7$ and 1.0 for $\zeta_{(sp)} = 2.0$. The amplitude of the higher mode oscillation has been increased to a magnitude that visible in the response.

The two systems were tested under slightly different conditions. Due to the difficulty in introducing a step input to the system by means of the torque generator of the gyro, it was determined that the sharpest input occurred when the controlled member was displaced by hand and then released. This method essentially introduced an initial angle of the controlled member with the input zero.

In the instance of the analog computer arrangement a step input to the system was used. This method caused the system to receive an initial kick from the frequency dependent term operating on the input. Equation Summary 4, equation (5). This difference probably accounts for the faster rise times of the predicted responses. It is believed that the difference in testing procedure did not materially effect the responses and that they are comparable. Both the analog computer solutions and the responses of the stable platform substantiate the behavior predicted from the theory.

CHAPTER 6

CONCLUSIONS AND RECOMMENDATIONS

The use of the damping servomechanism to provide damping for direct-drive stable platforms was demonstrated to be highly successful. Satisfactory damping was obtained for a wide range of frequency ratios, and damping ratios of the damping servo and the stable platform.

For adequate damping over the whole range of damping ratios of the stable platform, the ratio of the undamped natural frequency of the damping servo to the undamped natural frequency of the stable platform must be at least nine. However, for damping ratios of $\zeta_{(sp)} = 1.0$ or less a frequency ratio of six is adequate.

The frequency ratio, $\beta_{(ds)}$, available in the stable platform tested was limited due to the stiffness obtainable for the damping servo loop. It was evident that much higher frequency ratios could be obtained by better construction and phasing in the damping servomechanism. Using this method of damping, the stiffness of the stable platform may be increased as high as desired. The damping ratio of the stable platform will increase as the undamped natural frequency of the stable platform is increased. Ample damping will be available so long as the stiffness of the damping servomechanism can be increased to maintain the required frequency ratio, $\beta_{(ds)}$.

The stable platform loop used in the experiment contained a demodulator and a remodulator section which were necessary in order use a d. c. lead network for damping. However, with the

damping servomechanism the system may be made entirely a.c., resulting in a much simpler system. The damping servomechanism may be adopted to an all d.c. network by the addition of a demodulator on the tachometer output voltage as was done in the system tested.

The damping servomechanism has many advantages over other methods of damping. The damping servomechanism introduces no interferences due to base motion into the system. The damping servomechanism requires only electrical connection with the stable platform and need not be included in the inertial package. The damping servomechanism filters out all noise present in the correction signal of frequencies above the undamped natural frequency of the damping servomechanism.

It is recommended that further experimentation be done to determine, from the practical point of view, the upper limit of the undamped natural frequency of a damping servomechanism of this type. A more thorough analysis of the performance equations of the system is indicated to determine accurately the relationship between the variables $\zeta_{(ds)}$, $\zeta_{(sp)}$, and $\beta_{(ds)}$ and their effect on the performance of the system.

APPENDIX A

DERIVATION OF THE PERFORMANCE EQUATIONS FOR THE STABLE PLATFORM

Equation Summary 1.

Performance equation for a direct-drive single-axis stable platform employing a single degree of freedom floated integrating gyro. Fig. A-2 is a functional diagram of the system.

$$\left(I_{(cm)}\, p^2 + \left[S_{(tm)} \left[\dot{A};M\right]_{(sp)} + C_{(cm)_{(sp)}}\right] p + S_{(tm)} \left[i;M\right]_{(sp)} \left[PF\right]_{(dpcs)_{[e;i]_{(sp)}}} \left[PF\right]_{(igu)} \left[A;e\right]\right) A\left[I-(cm)\right]$$

$$= M_{(intfr)_{(cm)}} + \left[S_{(tm)} \left[\dot{A},M\right]_{(sp)} + C_{(cm)_{(sp)}}\right] p\, A\left[I-(ca)\right]$$

$$+ \left[PF\right]_{(igu)}\left[i;e\right] \left[PF\right]_{(dpcs)} \left[e;i\right]_{(sp)} S_{(tm)} \left[i;M\right]_{(sp)}{}^{1}(t\ k) \quad * \qquad (A\text{-}1)$$

$A\left[I-(cm)\right]$ = angular displacement of the controlled member with respect to the inertial space orientation for which the gyro output signal has its null level.

$I_{(cm)}$ = moment of inertia of the controlled member about the input axis. This includes the torque motor rotor, the platform, and the gyro unit.

---

*Adapted from equation (A-1) of equation summary (1) of reference 1. The notation adopted is self-defining in accordance with the generalized conventions given by Draper, McKay, and Lees in reference 5 Vol. 1.

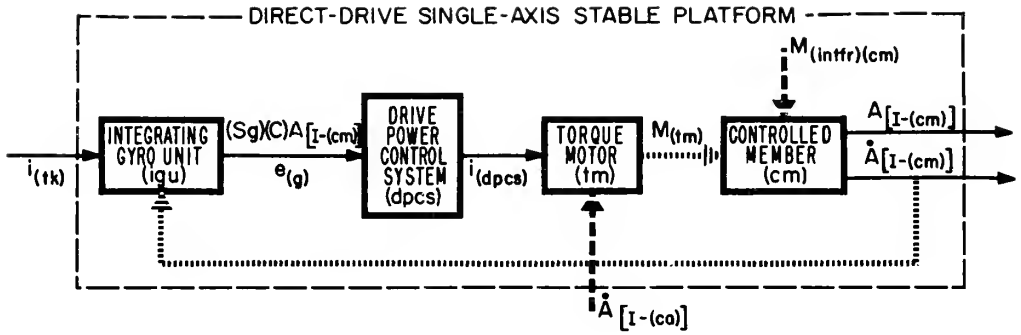

$i_{(tg)}$ = input current to torque generator on the output axis of the gyro unit

$A_{[I-(cm)]}$ = angular displacement of the controlled member with respect to the inertial space orientation for which the gyro output signal has its null level

$(Sg)(C)A_{[I-(cm)]} = e_{(g)}$ = correction signal voltage

$i_{(dpcs)}$ = output current of drive power control system

$M_{(tm)}$ = output torque of torque motor

$M_{(intfr)(cm)}$ = interference torque on the controlled member

$A_{[I-(ca)]}$ = angular displacement of the case with respect to the inertial space orientation for which the gyro output signal has its null level.

Fig. A-2 - Functional diagram for a single-axis direct-drive stable platform employing a single degree of freedom integration gyro unit

$S_{(tm)}\left[\dot{A};M\right]_{(sp)}$ = angular velocity input-torque output sensitivity magnitude of stable platform drive motor, i.e., motor damping.

$C_{(cm)_{(sp)}}$ = coefficient of viscous damping acting on the controlled member.

$S_{(tm)}\left[i;M\right]_{(sp)}$ = current input - torque output static sensitivity of stable platform drive motor.

$PF_{(dpcs)}\left[e;i\right]_{(sp)}$ = voltage input - current output performance function of the stable platform drive power control system $= S_{(dpcs)}\left[e;i\right]_{(sp)}{}^{(FF)}{}_{(dpcs)}\left[e;i\right]_{(sp)}$

$S_{(dpcs)}\left[e;i\right]_{(sp)}$ = voltage input - current output reference sensitivity of the stable platform drive power control system.

$(FF)_{(dpcs)}\left[e;i\right]_{(sp)}$ = voltage input-current output frequency function of the stable platform drive power control system. When frequency $\rightarrow 0$, $(FF)_{(dpcs)_{(sp)}} \rightarrow 1$.

$PF_{(igu)}\left[A;e\right]$ = $S_{(igu)\ A;e}\ {}^{(FF)}{}_{(igu)\ A;e}$ angle input-voltage output performance function of the gyro unit.

$S_{(igu)}\left[A;e\right]$ = angle input-voltage output sensitivity of the gyro unit.

$(FF)_{(igu)}\left[A;e\right]$ = angle input-voltage output frequency function of the gyro unit. When frequency $\rightarrow 0$, $(FF)_{(igu)\ A;e} \rightarrow 1$.

$M_{(intfr)_{(cm)}}$ = interference torque acting on the controlled member about the input axis.

$PF_{(igu)[i;e]}$ = current input-voltage output performance function of the gyro unit
$S_{(igu\ i;e}\ (FF)_{(igu)\ i;e}$

$S_{(igu)[i;e]}$ = current input-voltage output sensitivity of the gyro unit.

$(FF)_{(igu)[i,e]}$ = current input-voltage output frequency function of the gyro unit. When frequency → 0 $(FF)_{(igu)\ i;e} \rightarrow 1$.

$A\left[I - (ca)\right]$ = angular displacement of the case to which the stable platform drive motor stator is attached relative to the inertial reference orientation for which the gyro output signal has its null level.

a) Performance equation of a direct-drive single-axis stable platform employing an integrating gyro unit if the forcing frequency is low enough to consider the frequency dependent functions associated with the integrating gyro and the drive power control system equal to unity.

$$\left(I_{(cm)}\ p^2 + \left[S_{(tm)}\left[\dot{A};M\right]_{(sp)} + C_{(cm)_{(sp)}}\right] p + S_{(tm)}\left[i;M\right]_{(sp)}\ S_{(dpcs)[e\ i]_{(sp)}}\ S_{(igu)}\left[A;e\right]\right) A\left[1-(cm)\right]$$

$$= M_{(intfr)_{(cm)}} + \left[S_{(tm)}\left[\dot{A}\ M\right]_{(sp)} + C_{(cm)_{(sp)}}\right] p\ A\left[I-ca\right] + S_{(igu)[i;e]}\ S_{(dpcs)[e;i]_{(sp)}}\ S_{(tm)}\left[i;M\right]_{(sp)}\ {}^{1}(tk) \qquad (A\text{-}2)$$

$$\left(I_{(cm)}\ p^2 + S_{(sp)}\left[\dot{A};M\right]_{(res)}\ p + S_{(sp)}\left[A\ M\right]\right) A\left[1-(cm)\right]$$

$$= M_{(intfr)_{(cm)}} + S_{(sp)}\left[\dot{A}\ M\right]_{(res)}\ p\ A\left[I,(ca)\right] + S_{(sp)}\left[i,M\right]^{1}(tk) \qquad (A\text{-}3)$$

$S_{(tm)}\left[\dot{A};M\right]_{(sp)} + C_{(cm)(sp)} = S_{(sp)}\left[\dot{A};M\right]_{(res)}$ = angular velocity input-torque output sensitivity of the stable platform servo drive loop resulting from motor damping and viscous frictions on the controlled member.

$S_{(tm)}\left[i;M\right]_{(sp)} S_{(dpcs)}\left[e;i\right]_{(sp)} S_{(igu)}\left[A;e\right] = S_{(sp)}\left[A;M\right]$ = angle input-torque output sensitivity of the stable platform servo drive loop.

$S_{(igu)}\left[i;e\right] S_{(dpcs)}\left[e,i\right]_{(sp)} S_{(tm)}\left[i;M\right]_{(sp)} = S_{(sp)}\left[i;M\right]$ = current input-torque output sensitivity of the stable platform servo drive loop.

b) Parametric form of performance equation for a direct-drive single-axis stable platform employing an integrating gyro unit with gyro frequency functions equal to unity.

$$\left(\frac{p^2}{\omega_{n_{(sp)}}^2} + \frac{2\zeta_{(sp)(res)}}{\omega_{n_{(sp)}}} p + 1\right) A\left[I\text{-}(cm)\right] = S_{(sp)}\left[M;A\right] M_{(intfr)} + S_{(sp)}\left[\dot{A};A\right] p\, A_{I\text{-}(ca)} + S_{(sp)}\left[i;A\right] i_{(tk)} \qquad (A\text{-}4)$$

$\omega_{n_{(sp)}} = \sqrt{\dfrac{S_{(sp)}\left[A;M\right]}{I_{(cm)}}}$ = the natural undamped circular frequency of the stable platform servo drive loop.

$\zeta_{(sp)(res)} = \sqrt{\dfrac{S_{(sp)}\left[\dot{A};M\right]_{(res)}}{2\, I_{(cm)} S_{(sp)}\left[A;M\right]}}$ residual damping ratio of the stable platform servo drive loop due to motor damping and viscous friction acting on the controlled member.

$$S_{(sp)}\left[M;A\right] = \frac{1}{S_{(sp)}\left[A;M\right]}$$

$$S_{(sp)}\left[\dot{A};A\right] = \frac{S_{(sp)}\left[\dot{A};M\right]}{S_{(sp)}\left[A;M\right]}$$

$$S_{(sp)}\left[i;A\right] = \frac{S_{(sp)}\left[i;M\right]}{S_{(sp)}\left[A;M\right]}$$

Equation Summary 2.

Performance equation for a case-damped direct-drive single-axis stable platform employing a single-degree-of-freedom integrating gyro.

See Fig. 3 for a functional diagram of the system.

From equation summary 1 (a), equation A-1-3)

$$\left(I_{(cm)}\,p^2 + S_{(sp)}\left[\dot{A};M\right](res)\,p + S_{(sp)}\left[A;M\right]\right) A_{I-(cm)}$$

$$= M_{(intfr)(cm)} + S_{(sp)}\left[\dot{A};M\right](res)\,p\,A\left[I-(ca)\right] + S_{(sp)}\left[i;M\right]I_{(tk)} \qquad (A\text{-}2\text{-}1)$$

From Fig. 3 the damping signal = $e_{(t)}$

$$e_{(t)} = S_{(t)}\left[\dot{A};e\right](sp)\,p\,A\left[(ca),(cm)\right]$$

$$= S_{(t)}\left[\dot{A};e\right](sp)\,p\left(A\left[I-(cm)\right] - A\left[I-(ca)\right]\right) \qquad (A\text{-}2\text{-}2)$$

$e_{(t)}$ = output voltage of the tachometer

$S_{(t)}\left[\dot{A};e\right](sp)$ = angular velocity input-voltage output sensitivity of the stable platform drive loop tachometer

$A\left[(cm)-(ca)\right]$ = angular displacement of the case to which

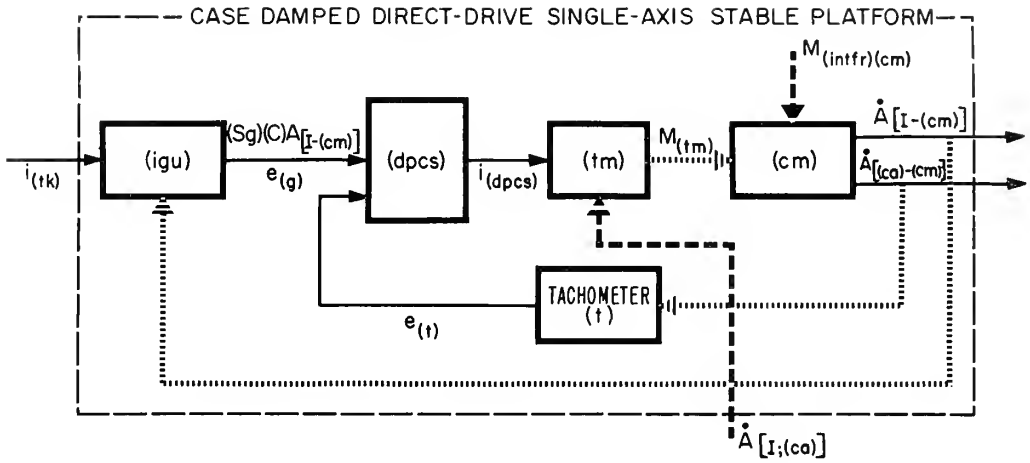

$e_{(t)}$ = output voltage of the tachometer

$A_{[(ca)-(cm)]} = A_{[I-(cm)]} - A_{[I-(ca)]}$ = angular velocity of the control member relative to the case on which the torque motor and the tachometer are mounted

Fig. A-3 Functional diagram of a case-damped direct-drive single-axis stable platform

$$\omega_{n_{(sp)}} = \sqrt{\frac{S_{(sp)}\left[A;M\right]}{I_{(cm)}}}$$

$$\zeta_{(sp)(res)} = \frac{1}{2} \frac{S_{(sp)}\left[\dot{A};M\right](res)}{\sqrt{I_{(cm)}\, S_{(sp)}\left[A;M\right]}}$$

$$\zeta_{(sp)} = \frac{1}{2} \frac{S_{(sp)}\left[\dot{A};M\right]}{\sqrt{I_{(cm)}\, S_{(sp)}\left[A;M\right]}}$$

Equation Summary 3*

Performance equations for a lead-modifier damped direct-drive single-axis stable platform employing a single-degree-of-freedom integrating gyro. See Fig. 5 for functional diagrams of the system.

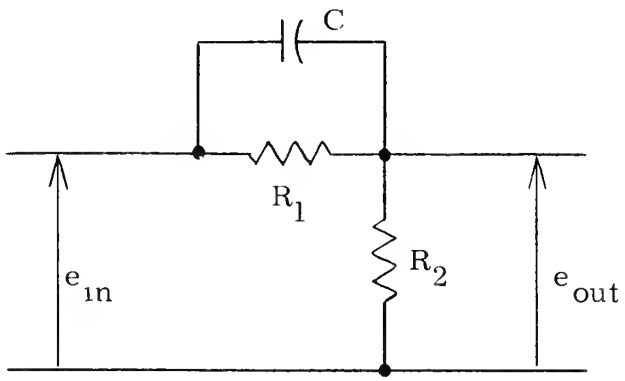

Fig. A-4 Typical lead modifier circuit

*Equation summary is taken from Ref. (4) and adapted to the stable platform.

$$\frac{e_{out}}{e_{in}} = [PF]_{ld} = S_{ld} \frac{1 + \nu_{ld}\,\tau_{ld}\,p}{1 + \tau_{ld}\,p} \quad , \ \nu_{ld} > 1 \qquad \text{(A-3-1)}$$

$$S_{ld} = \frac{R_2}{R_1 + R_2} = \frac{1}{\nu_{ld}} = \text{lead modifier sensitivity}$$

$$\tau_{ld} = \frac{R_2}{R_1 + R_2}$$

$$\nu_{ld} = \frac{R_1 + R_2}{R_2} = \text{lead modifier characteristic time ratio}$$

Referring back to equation summary 1 (a) equation 2 it is noted that the lead modifier network in the system, Fig. 5, modifies the sensitivity assigned to the drive power control system, $S_{(dpcs)\,[e;i]\,(sp)}$ as follows:

$$[PF]_{(dpcs)[e;i](sp)(cm)} = S_{ld} \frac{1 + \nu_{ld}\,\tau_{ld}\,p}{1 + \tau_{ld}\,p}\, S_{(dpcs)[e;i](sp)} \qquad \text{(A-3-2)}$$

$$= [PF]_{ld}\, S_{(dpcs)[e;i](sp)}$$

= voltage input–current output performance function of the stable platform servo drive system with lead modification.

Substitution of (A-3-2) for $S_{(dpcs)[e;i](sp)}$ in equation (A-3-2) of equation summary 1 (a) and reducing the result to the form of equation (A-3-3) of equation summary 1 (a)

$$\left(I_{(cm)}\,p^2 + S_{(sp)}[A;M]_{(res)}\,p + \frac{S_{ld}\,1 + \nu_{ld}\,\tau_{ld}\,p}{1 + \tau_{ld}\,p}\, S_{(sp)}[A;M]\right) A[I\text{-}(cm)]$$

$$= M_{(intfr)(cm)} + S_{(sp)}[A;M]_{(res)}\,p\,A[I\text{-}(ca)]$$

$$+ S_{ld} \frac{1 + \nu_{ld}\,\tau_{ld}\,p}{1 + \tau_{ld}}\, S_{(sp)}[i;M]^{i}_{(tk)} \qquad \text{(A-3-3)}$$

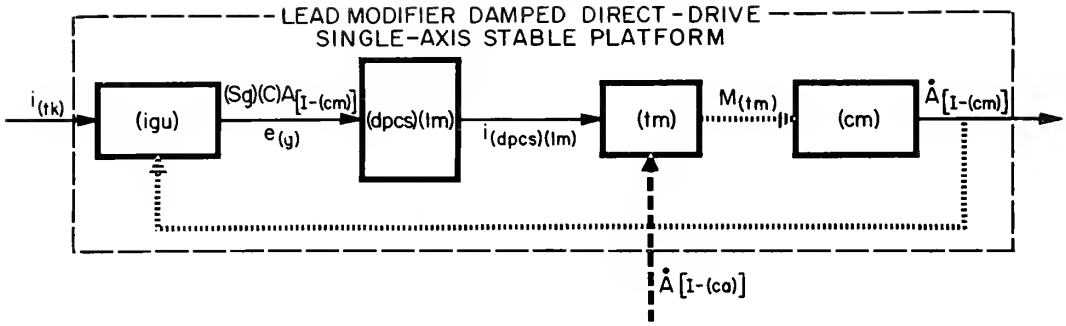

(dpcs)(lm) = lead modified drive power control system

$i_{(dpcs)(lm)}$ = output current of lead modified drive power control system

Fig. A-5 Functional diagram of a lead modifier damped direct-drive single-axis stable platform

the tachometer stator is attached relative to the angular position of the controlled member.

The voltage $e_{(t)}$ creates a torque on the controlled member

$$M_{(d)(sp)} = S_{(t)}\left[\dot{A};e\right](sp)\, S_{(dpcs)}[e;i](sp)\, S_{(tm)}\left[i;M\right](sp)\dot{A}\left[(cm)-(ca)\right]$$

$$= S_{(sp)}\left[\dot{A};M\right]\left[\dot{A}\, I\text{-}(cm) - A\left[I\text{-}(ca)\right]\right] \qquad (A\text{-}2\text{-}3)$$

$M_{(d)(sp)}$ = damping torque at the controlled member provided by the tachometer.

$S_{(t)}\left[\dot{A};e\right](sp)\, S_{(dpcs)}\left[e;i\right](sp)\, S_{(tm)}\left[i;M\right](sp) = S_{(sp)}\left[\dot{A};M\right]$ = angular velocity input-torque output sensitivity of the stable platform servo drive loop.

Including the damping torque in equation (A-2-1) results in

$$\left(I_{(cm)}\, p^2 + \left[S_{(sp)}\left[\dot{A};M\right] + S_{(sp)}\left[\dot{A};M\right](res)\right]p + S_{(sp)}\left[A;M\right]\right)A\left[I\text{-}(cm)\right] =$$

$$M_{(intfr)(cm)} + \left(S_{(sp)}\left[\dot{A};M\right] + S_{(sp)}\left[\dot{A};M\right](res)\right) p\, A\left[I\text{-}(ca)\right] +$$

$$+ S_{(sp)}\left[i;M\right]\, i_{(tk)} \qquad (A\text{-}2\text{-}4)$$

Writing equation (A-2-4) in parametric form

$$\left(\frac{p^2}{\omega_{n_{(sp)}}^2} + \left[\frac{2\,\zeta_{(sp)}}{\omega_{n_{(sp)}}} + \frac{2\zeta_{(sp)(res)}}{\omega_{n_{(sp)}}}\right] p + 1\right) A\left[I\text{-}(cm)\right] =$$

$$S_{(sp)}\left[M;A\right]\, M_{(intfr)(cm)} + \left(S_{(sp)}\left[\dot{A};A\right] + S_{(sp)}\left[\dot{A};A\right](res)\right) p\, A\left[I\text{-}(ca)\right]$$

$$+ S_{(sp)}\left[i;A\right]\, i_{(tk)} \qquad (A\text{-}2\text{-}5)$$

a) Parametric form of performance equation for a lead-modifier damped direct-drive single-axis stable platform.

$$\left(\frac{p^2}{\omega^2_{n_{(sp)}}} + \frac{2\zeta_{(sp)(res)}}{\omega_{n_{(sp)}}} p + S_{ld}\ \frac{1+\nu_{ld}\,\tau_{ld}\,p}{1+\tau_{ld}\,p}\right) A\left[I-(cm)\right] =$$

$$S_{(ps)}\left[M;A\right] M_{(intfr)(cm)} + S_{(sp)}\left[\dot{A};A\right]_{(res)}\, p\, A\left[I-(ca)\right]$$

$$+ S_{ld}\,\frac{1+\nu_{ld}\,\tau_{ld}\,p}{1+\tau_{ld}\,p}\, S_{(ps)}\left[i;A\right] {}^{i}(tk) \qquad \text{(A-3-4)}$$

Equation (A-3-4(may be rewritten as

$$\left[\frac{\nu_{ld}\,\tau_{ld}\,p}{1+\nu_{ld}\,\tau_{ld}\,p}\left(\frac{p^2}{\omega^2_{n_{(sp)}}} + \frac{2\zeta_{(sp)(res)}}{\omega_{n_{(sp)}}} p\right)\right.$$

$$\left. + \frac{\nu_{ld}}{1+\nu_{ld}\,\tau_{ld}\,p}\, p\left(\frac{p}{\omega^2_{n_{(sp)}}} + \frac{2\zeta_{(sp)(res)}}{\omega_{n_{(ps)}}}\right) + 1\right] A\left[I-(cm)\right]$$

$$= \nu_{ld}\,\frac{1+\tau_{ld}\,p}{1+\nu_{ld}\,\tau_{ld}\,p}\, S_{(sp)}\left[M;A\right] M_{(intfr)(cm)}$$

$$+ \nu_{ld}\,\frac{1+\tau_{ld}\,p}{1+\nu_{ld}\,\tau_{ld}\,p}\, S_{(sp)}\left[\dot{A},A\right]_{(res)}\, p\, A\left[I-(ca)\right]$$

$$+ S_{(sp)}\left[i;A\right]^{1}(tk) \qquad \text{(A-3-5)}$$

Replacing the operator p with $j\omega_f$

$$\nu_{ld}\ \frac{1+\tau_{ld}\,j\omega_f}{1+\nu_{ld}\,\tau_{ld}\,j\omega_f} = \frac{\nu_{ld}}{1+\nu_{ld}\,\tau_{ld}} + \frac{\nu_{ld}\,\tau_{ld}\,j\,\omega_f}{1+\nu_{ld}\,\tau_{ld}\,j\omega_f} \qquad \text{(A-3-6)}$$

For small values of the forcing frequency, (A-3-6) is equal to ν_{ld}, and as the forcing frequency gets large (A-3-6) approaches unity.

Using this characteristic of (A-3-6) the approximate performance equation for low forcing frequencies is

$$\left[\nu_{ld}\left(\frac{p^2}{\omega^2_{n_{(sp)}}} + \frac{2\zeta_{(sp)(res)}p}{\omega_{n_{(sp)}}}\right) + 1\right] A\left[\bar{I}\text{-}(cm)\right] =$$

$$\nu_{ld}\, S_{(sp)}\left[M;A\right] M_{(intfr)(cm)} + \nu_{ld}\, S_{(sp)}\left[\dot{A};A\right]_{(res)} p\, A\left[\bar{I}\text{-}(ca)\right]$$

$$+ S_{(sp)}\left[i;A\right]^{1}(tk) \qquad \text{(A-3-7)}$$

For intermediate frequencies the approximation is

$$\left[\frac{p^2}{\omega^2_{n_{(sp)}}} + 2\zeta_{(sp)(res)}\frac{p}{\omega_{n_{(sp)}}} + \frac{p}{\tau_{ld}\,\omega^2_{n_{(sp)}}} + \frac{2\zeta_{(sp)(res)}}{\tau_{ld}\,\omega_{n_{(sp)}}} + 1\right] A\left[\bar{I}\text{-}(cm)\right]$$

$$= \left(1 + \frac{1}{\tau_{ld}\,p}\right) S_{(ps)}\left[M;A\right] M_{(intfr)(cm)}$$

$$+ \left(1 + \frac{1}{\tau_{ld}\,p}\right) S_{(sp)}\left[A;A\right]_{(res)}\, p\, A\left[\bar{I}\text{-}(ca)\right]$$

$$+ S_{(sp)}\left[i;A\right]\, i_{(tk)} \qquad \text{(A-3-8)}$$

For high frequencies the approximation is

$$\left[\frac{p^2}{\omega^2_{n_{(sp)}}} + 2\zeta_{(sp)(res)}\frac{p}{\omega_{n_{(sp)}}} + 1\right] A\left[\bar{I}\text{-}(cm)\right]$$

$$= S_{(sp)}\left[M;A\right] M_{(intfr)(cm)} + S_{(sp)}\left[\dot{A};A\right] pA\left[\bar{I}\text{-}(ca)\right]$$

$$+ S_{(sp)}\left[i;A\right]\, i_{(tk)} \qquad \text{(A-3-9)}$$

Derivation Summary 1

The performance equation for space-damped direct-drive single-axis stable platform. The damping signal is provided by a second-order closed loop servomechanism as shown functionally in Fig. 6.

The performance equation for the damping servomechanism is

$$\left[I_{(dcm)}\, p^2\, A\left[I\text{-}(dcm)\right] + \left(S_{(dtm)}\left[\dot{A},M\right](ds) + C_{(dcm)(ds)} + S_{(dt)}\left[\dot{A};e\right](ds)\left[PF\right]_{(dpcs)\left[e;i\right](ds)} S_{(dtm)}\left[i;M\right] \right) p\, A_{(ca)\text{-}(dcm)} + S_{(dsg)}\left[A;e\right](ds)\left[PF\right]_{(dpcs)\left[e;i\right](ds)} S_{(dtm)}\left[i;M\right](ds) \right] A\left[(ca)\text{-}(dcm)\right] = M_{(intfr)(dcm)} + \left[PF\right]_{(dpcs)\left[e;i\right](ds)} S_{(dtm)}\left[i;M\right](ds)\,(Sg)(C)A\left[I\text{-}(cm)\right](sp) \qquad (A\text{-}1\text{-}1)$$

$$A\left[I\text{-}(dcm)\right] = A\left[(ca)\text{-}(cm)\right] + A\left[I\text{-}(ca)\right]$$

= angular displacement of the damper controlled member with respect to an inertial space orientation.

$A\left[(ca)\text{-}(dcm)\right]$ = angular displacement of the damper controlled member with respect to the case, i.e., the stator case of the damper torque motor.

$S_{(dt)}\left[\dot{A};e\right](ds)$ = angular velocity input-voltage output of the damping servomechanism tachometer.

$(Sg)(C)A\left[I\text{-}(cm)\right](sp) = S_{(igu)}\left[A,e\right] A\left[I\text{-}(cm)\right](sp) = e_g$

= correction signal voltage from the stable platform servo drive loop.

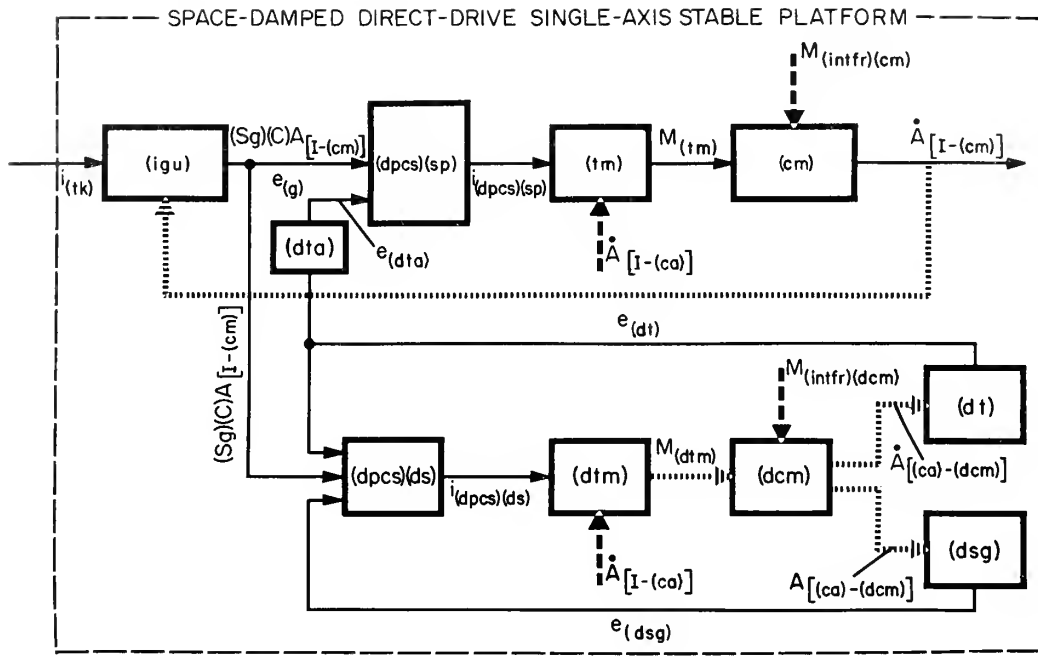

(dpcs)(sp)	=	stable platform drive power control system
(dpcs)(ds)	=	damping servomechanism drive power control system
(dtm)	=	damper torque motor
(dcm)	=	damper controlled member
(dt)	=	damper tachometer
(dsg)	=	damper signal generator
(dta)	=	damper tachometer amplifier

Fig. A-6 Functional diagram for a space-damped direct-drive single-axis stable platform

a) The performance equation for the damping-servo if the forcing frequency is low enough to consider the frequency depenent function of the damping-servo drive power control system equal to unity. Also considering $I_{(dcm)}\ddot{A}\,[\bar{I}-(ca)]$ as an interference input and arranging the coefficients as in equation summary 1(a), equation (A-1-3)

$$\left(I_{(dcm)}p^2 + \left[S_{(ds)[\dot{A};M](res)} + S_{(ds)[\dot{A};M]}\right]p + S_{(ds)[A;M]}\right)A_{[(ca)-(dcm)]}$$

$$= M_{(intfr)(dcm)} + S_{(ds)[e;M]}\,(Sg(C)A_{[\bar{I}-(cm)](sp)} - I_{(dcm)}p^2\,A_{[\bar{I}-(ca)](ds)} \qquad \text{(A-1-2)}$$

Writing equation (A-1-2) in parametric form gives

$$\left(\frac{p^2}{\omega_{n}^{2}_{(ds)}} + \left(\frac{2\zeta_{(ds)(res)}}{\omega_{n(ds)}} + \frac{2\zeta_{(ds)}}{\omega_{n(ds)}}\right)p + 1\right)A_{[(ca)-(dcm)]} =$$

$$S_{(ds)[M;A]}M_{(intfr)(dcm)} + S_{(ds)[e;A]}(Sg)(C)A_{[\bar{I}-(cm)](sp)}$$

$$- \frac{p^2}{\omega_{n}^{2}_{(ds)}}\,A_{[\bar{I}-(ca)]} \qquad \text{(A-1-3)}$$

$S_{(ds)[e;A]} = \dfrac{S_{(ds)[e;M]}}{S_{(ds)[A;M]}}$ = voltage input-angle output sensitivity of the damping servo loop.

b) The damper-tachometer-amplifier output voltage is used as a damping signal for the stable platform servo drive loop. The functions that make up the damper-tachometer-amplifier output voltage may be arranged as follows

$$e_{(dta)} = S_{(dta)[e;e](ds)}\,e_{(di)} \qquad \text{(A-1-4)}$$

$S_{(dta)[e;e](ds)}$ = voltage input-voltage output sensitivity of the damper-tachometer-amplifier.

$$e_{(dta)} = S_{(dta)[e;e](ds)} S_{(dt)[\dot{A};e](ds)} p A_{[(ca)-(cm)]} \qquad (A\text{-}1\text{-}5)$$

Solving $A_{[(ca)-(cm)]}$ from equation (A-1-2) and substituting in equation (A-1-5)

$$e_{(dta)} = \frac{S_{(dta)[e;e](ds)} S_{(dt)[\dot{A};e](ds)} p \left(M_{(intfr)(dcm)} + S_{(ds)[e;M]} (Sg)(C) A_{[I-(cm)](sp)} - I_{(dcm)} p^2 \ddot{A}_{[I-(ca)](ds)} \right)}{I_{(dcm)} p^2 + S_{(ds)[\dot{A};M](res)} + S_{(ds)[\dot{A};M]} p + S_{(ds)[A;M]}}$$

(A-1-6)

The residual damping torque present in the damping servo is useful and makes no contribution to the static errors. It will be included in the tachometer feedback damping torque, $S_{(ds)[\dot{A};M]} p A_{[(ca)-(cm)]}$, in the following equations.

If the inertia of the damper controlled member is extremely small and the gain of the damping servo loop is high, then even if the angular acceleration of the case relative to inertial space is large $- I_{(dcm)} p^2 \ddot{A}_{[I-(ca)](ds)}$ may be ignored as a second order torque. This term will not be included in the following equations.

The interferenece torque acting on the damper control member, $M_{(intfr)(dcm)}$, can be negligible if there is no load acting on the controlled member except the friction of the damper signal generator which can be made quite small.

Dropping the interference inputs from equation (A-1-6) and including $S_{(ds)[\dot{A};M](res)}$ in the term $S_{(ds)[\dot{A};M]}$

$$e_{(dta)} = \frac{\left[S_{(dta)[e;e](ds)} S_{(dt)[\dot{A};e](ds)} S_{(ds)[e;M]} \right] p (Sg)(C) A_{[I-(cm)](sp)}}{I_{(dcm)} p^2 + S_{(ds)[\dot{A};M]} p + S_{(ds)[A;M]}}$$

(A-1-7)

$S_{(dt)}\left[\dot{A};e\right]S_{(ds)}\left[e;M\right] = S_{(ds)}\left[\dot{A};M\right]$ = angular velocity input-torque output sensitivity of the damping servo loop

$$(Sg)(C)A\left[I-(cm)\right](sp) = S_{(igu)}\left[A;e\right]A\left[I-(cm)\right](sp)$$

$$e_{(dta)} = \frac{S_{(dta)}\left[e;e\right](ds)S_{(ds)}\left[\dot{A},M\right]S_{(igu)}\left[A;e\right]p\,A\left[I-(cm)\right](sp)}{I_{(dcm)}\,p^2 + S_{(ds)}\left[\dot{A};M\right]p + S_{(ds)}\left[A;M\right]} \qquad (A\text{-}1\text{-}8)$$

Or writing equation (A-1-8) in parametric form

$$e_{(dta)} = \frac{S_{(dta)}\left[e;e\right](ds)S_{(ds)}\left[\dot{A};A\right]S_{(igu)}\left[A;e\right]p\,A\left[I-(cm)\right](sp)}{\frac{p^2}{\omega_{n_{(ds)}}^2} + \frac{2\zeta_{(ds)}}{\omega_{n_{(ds)}}}\,p + 1} \qquad (A\text{-}1\text{-}9)$$

c) The performace equation of the direct-drive single-axis stable platform with space-damping.

The damper-tachometer-amplifier output voltage used as a damping signal for the stable platform servo drive loop puts a damping torque, $M_{(d)}$, on the controlled member.

$$M_{(d)} = S_{(sp)}\left[e;M\right]e_{(eta)} \qquad (A\text{-}1\text{-}10)$$

$S_{(sp)}\left[e;M\right] = S_{(dpcs)}\left[e;i\right](sp)\,S_{(tm)}\left[i;M\right](sp)$ = voltage input-torque output of the stable platform servo drive.

Substituting equation (A-1-8) for $e_{(eta)}$ in equation (A-1-10)
Setting $i_{(tk)} = 0$ for the present.

$$M_{(d)} = \frac{S_{(dpcs)}\left[e;i\right](sp)S_{(tm)}\left[i;M\right](sp)S_{(dta)}\left[e;e\right](ds)S_{(ds)}\left[\dot{A};M\right]S_{(igu)}\left[A;e\right]pA\left[I-(cm)\right](sp)}{I_{(dcm)}\,p^2 + S_{(ds)}\left[\dot{A};M\right]p + S_{(ds)}\left[A;M\right]} \qquad (A\text{-}1\text{-}11)$$

$S_{(dpcs)[e;i](sp)}\ S_{(tm)[i;M](sp)}\ S_{(igu)[A;e]} = S_{(sp)[A;M]}$ = angle input-torque output sensitivity of the stable platform servo drive loop.

The damping torque is put into equation (A-1-3) of equation summary 1(a).

$$\left(I_{(cm)}p^2 + \left[S_{(sp)[\dot{A};M](res)} + \frac{S_{(dta)[e;e](ds)}S_{(ds)[\dot{A};M]}S_{(sp)[A;M]}}{I_{(dcm)}p^2 + S_{(ds)[\dot{A};M]}p + S_{(ds)[A;M]}}\right]p + S_{(sp)[A;M]}\right) A[I-(cm)] = M_{(intfr)(cm)} + S_{(sp)[\dot{A};M](res)}\ p\ A[I-(ca)] \qquad (A\text{-}1\text{-}12)$$

Putting equation (A-1-12) in parametric form

$$\left(\frac{p^2}{\omega^2_{n_{(sp)}}} + \left[\frac{2\zeta_{(sp)(res)}}{\omega_{n_{(sp)}}} + \frac{\frac{2\zeta_{(sp)(res)}}{\omega_{n_{(sp)}}}}{\frac{p^2}{\omega^2_{n_{(ds)}}} + \frac{2\zeta_{(ds)}}{\omega_{n_{(ds)}}} + 1}\right]p + 1\right) A[I-(cm)]$$

$$= S_{(sp)[M;A]}M_{(intfr)(cm)} + S_{(sp)[\dot{A};A](res)}\ p\ A[I-(ca)] \qquad (A\text{-}1\text{-}13)$$

$$\omega_{n_{(sp)}} = \sqrt{\frac{S_{(sp)[A;M]}}{I_{(cm)}}} \qquad (A\text{-}1\text{-}14)$$

$$\zeta_{(sp)(res)} = \frac{1}{2}\frac{S_{(sp)[\dot{A};M](res)}}{\sqrt{I_{(cm)}S_{(sp)[A;M]}}} \qquad (A\text{-}1\text{-}15)$$

$$\zeta_{(sp)} = \frac{1}{2}\ S_{(dta)[e;e](ds)}S_{(ds)[\dot{A};A]}\sqrt{\frac{S_{(sp)[A;M]}}{I_{(cm)}}} \qquad (A\text{-}1\text{-}16)$$

$$S_{(ds)}\left[\dot{A};A\right] = \frac{S_{(dt)}\left[\dot{A};e\right](ds)}{S_{(dsg)}\left[A;e\right](ds)}$$

For $\omega_{n_{(ds)}}$ sufficiently large relative to p

$$\frac{p^2}{\omega_{n_{(ds)}}^2} + \frac{2\zeta_{(ds)}}{\omega_{n_{(ds)}}} p + 1 \doteq 1 \qquad \text{(A-1-17)}$$

equation (A-1-13) is now non dimensionalized by letting

$$'p = \frac{p}{\omega_{n_{(sp)}}}$$

and

$$\beta_{(ds)} = \frac{\omega_{n_{(ds)}}}{\omega_{n_{(sp)}}}$$

$$\left('p^2 + \left[2\zeta_{(sp)(res)} + \frac{2\zeta_{(sp)}}{\frac{'p^2}{\beta_{(ds)}^2} + \frac{2\zeta_{(ds)}\,'p}{\beta_{(ds)}} + 1}\right]'p + 1\right) A\left[I-(cm)\right] =$$

$$S_{(sp)}\left[M;A\right] M_{(intfr)(cm)} + S_{(sp)}\left[\dot{A};A\right](res)\,\omega_{n_{(sp)}}\,'p\,A\left[I-(ca)\right] \qquad \text{(A-1-18)}$$

$$\zeta_{(sp)} = \frac{1}{2}\,\frac{S_{(dta)}\left[e;e\right](ds)\,S_{(dt)}\left[\dot{A};e\right](ds)}{S_{(dsg)}\left[a;e\right](ds)}\,\omega_{n_{(sp)}} \qquad \text{(A-1-18a)}$$

If $i_{(tk)}$ is not zero then the right side of equation (A-1-14) is

$$S_{(sp)}\left[M;A\right] M_{(intfr)(cm)} + S_{(sp)}\left[\dot{A};A\right](res)\,\omega_{n_{(sp)}}\,'p\,A\left[I-(ca)\right]$$

$$+ S_{(sp)}\left[i;A\right] i_{(tk)} + \frac{S_{(dta)}\left[e;e\right](ds)\,S_{(ds)}\left[\dot{A};A\right]S_{(sp)}\left[i;A\right]\omega_{n_{(sp)}}\,'p\,i_{(tk)}}{\frac{'p^2}{\beta_{(ds)}^2} + \frac{2\zeta_{(ds)}}{\beta_{(ds)}}\,'p + 1} \qquad \text{(A-1-19)}$$

Equation Summary 4

Performance equation solved by analog computer to obtain predicted results. See Fig. 7.

Performance equation of the second-order system to be damped written in parametric form

$$\frac{p^2}{\omega_{n(sp)}^2} + 1 \quad A_{(cm)} = A_{(in)} \tag{A-4-1}$$

Performance equaton of the second order system used to provide a damping signal for equation (A-4-1)

$$\left(\frac{p^2}{\omega_{n(ds)}^2} + \frac{2\zeta_{(ds)}}{\omega_{n(ds)}} + 1 \right) A_{(dcm)} = (C)\, A_{(cm)} \tag{A-4-2}$$

$(C)\, A_{(cm)}$ = correction signal of equation (A-4-1)

Taking the derivation of both sides of equation (A-4-2) and rearranging it

$$p\, A_{(dcm)} = \frac{p\,(C)\, A_{(cm)}}{\frac{p^2}{\omega_{n(ds)}^2} + \frac{2\zeta_{(ds)}}{\omega_{n(ds)}} + 1} \tag{A-4-3}$$

If $p\, A_{dcm}$ is picked off the solution for the damping system and fed to the input of the second order system, equation (A-4-1), through an amplifier, the performance equation that results is

$$\left(\frac{p^2}{\omega_{n(sp)}^2} + \frac{S_a}{\frac{p^2}{\omega_{n(ds)}^2} + \frac{2\zeta_{(ds)}}{\omega_{n(ds)}} + 1}\, p + 1 \right) A_{(cm)} = \tag{A-4-4}$$

$$A_{(in)} + \frac{S_a\, p\, A_{(in)}}{\frac{p^2}{\omega_{n(ds)}^2} + \frac{2\zeta_{(ds)}}{\omega_{n(ds)}} + 1}$$

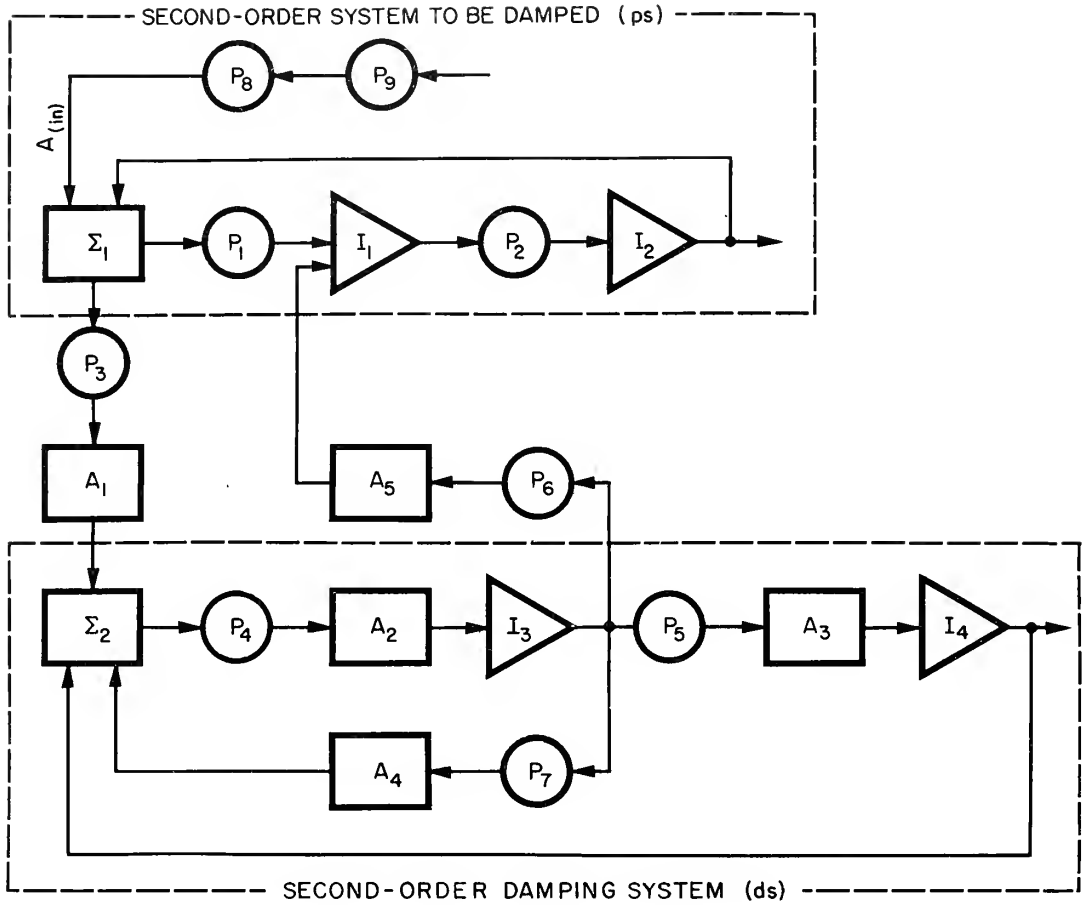

I = integrator

P = potentiometer

$\sum$ = summing amplifier

A = amplifier

Set $P_1 = P_2$

$P_4 = P_5$

$A_2 = A_3$

$S_{P_6} A_5 = 2 S_{P_1} \beta_{(ds)}$

$S_{\sum_1} = S_{\sum_2} = 1$

$$\zeta_{(ps)} = S_{P_3} S_{A_1}$$

$$\beta_{(ds)} = \frac{S_{P_4} S_{A_2}}{S_{P_1}}$$

$$\zeta_{(ds)} = \frac{S_{P_7} S_{A_4}}{2}$$

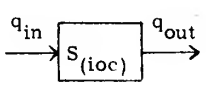

$S_{(ioc)} = \frac{q_{out}}{q_{in}}$ = sensitivity of identified component

Fig. A-7 Analog computer diagram of the system employed to obtain the predicted results

or nondimensionalizing by setting

$$'p = \frac{p}{\omega_{n_{(sp)}}} \qquad \text{and} \qquad \beta_{(ds)} = \frac{\omega_{n_{(ds)}}}{\omega_{n_{(sp)}}}$$

$$\left('p^2 + \frac{S_a\ \omega_{n_{(sp)}}}{\frac{'p^2}{\beta^2_{(ds)}} + \frac{2\zeta_{(ds)}\,'p}{\beta_{(ds)}} + 1}\,'p + 1\right) A_{cm} =$$

$$A_{in} + \frac{S_a\ \omega_{n_{(sp)}}\ 'p\ A_{in}}{\frac{p^2}{\beta^2_{(ds)}} + \frac{2\zeta_{(ds)}}{\beta_{(ds)}} + 1} \qquad \text{(A-4-5)}$$

$$\zeta_{(sp)} = \frac{\omega_{n_{(sp)}}\ S_a}{2}$$

Equation Summary 5

Approximate performance equation for Instrumentation Laboratory direct-drive single-axis stable platform with space damping by a high speed second-order servomechanism. Fig. A-8 is a functional diagram of the system.

Assumptions:

1. Motor damping and viscous friction of both the stable-platform and the damping servo are small and may be neglected.
2. Interference inputs to the damping servo are small and may be neglected.
3. The frequency functions associated with all electronic components are equal to unity for the forcing frequencies anticipated.

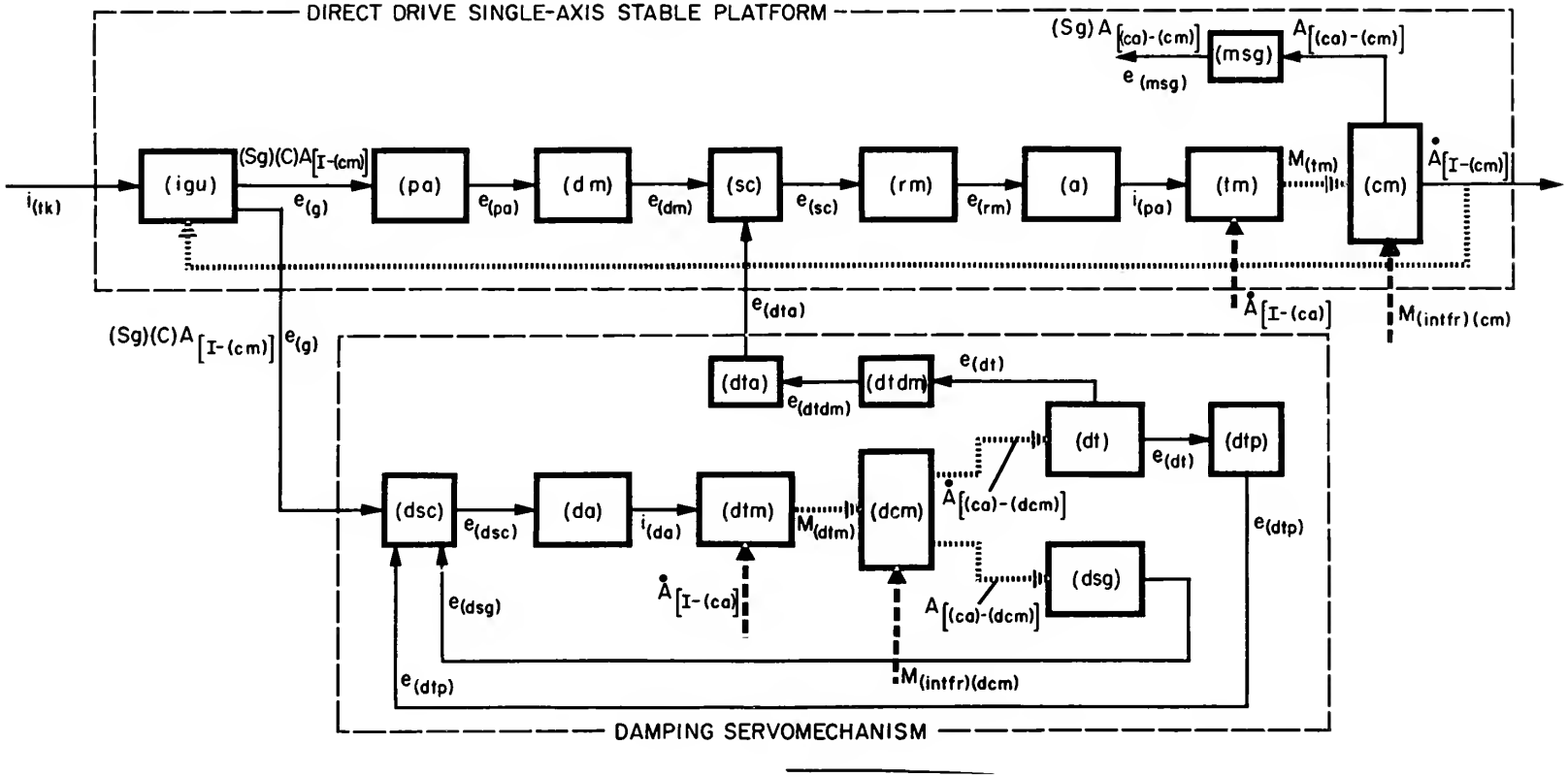

Fig. A-8 Functional diagram of the space-damped direct-drive single-axis stable platform used in the investigation

(pa) = pre-amplifier

(dm) = demodulator

(sc) = signal comparator

(rm) = remodulator

(a) = power amplifier

(tm) = torque motor

(cm) = controlled member

(msg) = microsyn signal generator

(dsc) = damper signal comparator

(da) = damper amplifier

(dtm) = damper torque motor

(dcm) = damper controlled member

(dt) = damper tachometer

(dsg) = damper signal generator

(dtp) = damper tachometer

(igu) = integrating gyro unit

$e_{(dsc)}$ = voltage output of the damper signal comparator

$i_{(da)}$ = current output of damper power amplifier

$M_{(dtm)}$ = torque output of the damper torque motor

$M_{(intfc)(dcm)}$ = interference torque on the damper controlled member

$i_{(tk)}$ = current input to torque generator on output axis of the gyro unit

$(S_g)(C)A_{I-(cm)} = e_{(g)}$ = correction signal voltage

$e_{(pa)}$ = voltage output of preamplifier

$e_{(dm)}$ = voltage output of demodulator

$e_{(sc)}$ = voltage output of signal comparator

$e_{(rm)}$ = voltage output of remodulator

$i_{(pa)}$ = current output of power amplifier

$M_{(tm)}$ = torque output of torque motor

$M_{(intfc)(cm)}$ = interference torque on the controlled member

$A_{I-(cm)}$ = angular displacement of the controlled member with respect to the inertial space orientation for which the gyro output voltage has its null value

$A_{(ca)-(cm)}$ = angular displacement of the controlled member with respect to the case, i.e., the torque motor stator

$(S_g)A_{(ca)-(cm)} = e_{(msg)}$ = voltage output of the microsyn signal generator

$A_{(ca)-(dm)}$ = angular displacement of the damper controlled member with respect to the case

$e_{(dt)}$ = voltage output of damper tachometer

$e_{(dsg)}$ = voltage output of damper signal generator

$e_{(dta)}$ = voltage output of damper tachometer amplifier

$e_{(dt\ dm)}$ = voltage output of the damper tachometer demodulator

Fig. A-8 Functional diagram of the space-damped direct-drive single-axis stable platform used in the investigation

Then follow the same procedure used to obtain equation (A-1-12) of derivation summary 1 (c), the performance equation of the system is

$$\left(I_{(cm)}p^2 + \frac{S_{(sc)}[e;e]\,(sp)\,S_{(dta)}[e;e]\,(ds)\,S_{(dtdm)}[e;e]\,(ds)\,S_{(ds)}[\dot{A},M]\,S_{(sp)}[A;M]}{I_{(dcm)}p^2 + S_{(ds)}[\dot{A};M]\,p + S_{(ds)}[A,M]}\,p\right.$$

$$\left. + S_{(sp)}[A;M]\right) A[I-(cm)] = M_{(intfr)(cm)} + S_{(sp)}[i;M]\,i_{(tk)} \qquad \text{(A-5-1)}$$

$$+ \frac{S_{(sc)}[e;e]\,(sp)\,S_{(dta)}[e;e]\,(ds)\,S_{(dtdm)}[e;e]\,(ds)\,S_{(ds)}[\dot{A},M]\,S_{(sp)}[i;M]\,p\,i_{(tk)}}{I_{(dcm)}p^2 + S_{(ds)}[\dot{A};M]\,p + S_{(ds)}[A;M]}$$

Terms not defined in Fig. A-8 are

$S_{(ds)}[\dot{A};M] = S_{(dt)}[\dot{A};e]\,S_{(dsc)}[e;e]\,S_{(da)}[e,i]\,S_{(dtm)}[i;M]$ = angular velocity input-torque output sensitivity of the damping servo

$S_{(ds)}[A;M] = S_{(dsg)}[A;e]\,S_{(dsc)}[e;e]\,S_{(da)}[e,i]\,S_{(dtm)}[i;M]$ = angular displacement input-torque output sensitivity of the damping servo

$S_{(sp)}[A;M] = (S_{(igu)}[A;e]\,S_{(pa)}[e;e]\,S_{(dm)}[e,e]\,S_{(sc)}[e,e])\,x$

$(S_{(rm)}[e,e]\,S_{(a)}[e,i]\,S_{(tm)}[i;M])$ = angular displacement input-torque output sensitivity of the stable platform

The left side of equation (A-5-1) written in parametric form is

$$\left(\frac{p^2}{\omega_{n_{(sp)}}} + \frac{\frac{2\zeta_{(sp)}}{\omega_{n_{(sp)}}}}{\frac{p^2}{\beta^2_{(ds)}} + \frac{2\zeta_{(ds)}}{\beta_{(ds)}} + 1} + 1\right) A[I-(cm)]$$

$$\omega_{n_{(sp)}} = \sqrt{\frac{S_{(sp)}\ [A;M]}{I_{(cm)}}}$$

$$\zeta_{(sp)} = \frac{\frac{1}{2}\ \frac{S_{(sc)}[e;e]\ (sp)\ S_{(dta)}[e;e]\ (ds)\ S_{(dtdm)}[e;e]\ (ds)\ S_{(dt)}[\dot{A};e]\ (ds)}{S_{(dsg)}[A;e]\ (ds)}}{\sqrt{\frac{I_{(cm)}}{S_{(sp)}[A;M]}}}$$

APPENDIX B

DESCRIPTION OF EQUIPMENT

Refer to Fig. A-8, B-1, B-2 and B-12 for the arrangement of the components in the stable platform and the damping servomechanism.

A 20 IG, 10^4, integrating gyro unit was used in the test.

The preamplifier, demodulator, remodulator, amplifier and necessary excitation sources were built up by the Instrumentation Laboratory personnel and installed in a test console , M.I.T. Laboratory No. 7202, pictures in Fig. B-1.

No frequency responses were run on the components in the console. The preamplifier-demodulator combination and the signal comparator-remodulator-amplifier combination were checked for linearity of static sensitivity. The static sensitivity curves appear in Fig. B-4 and B-5.

The torque motor was built to specifications of the Instrumentation Laboratory by the Inland Motor Corporation and designated the MT 5.1-104 motor. It is a two-phase, 400 cps, induction motor. The standstill characteristics of the motor are in Fig. B-6.

The microsyn signal generator voltage, proportional to the angular position of the controlled member, was recorded as the output. The voltage output of the microsyn was linear with input angle for the angular range used in the tests ($\pm 5^{\circ}$). Fig. B-7.

The damping servomechanism was constructed from spare

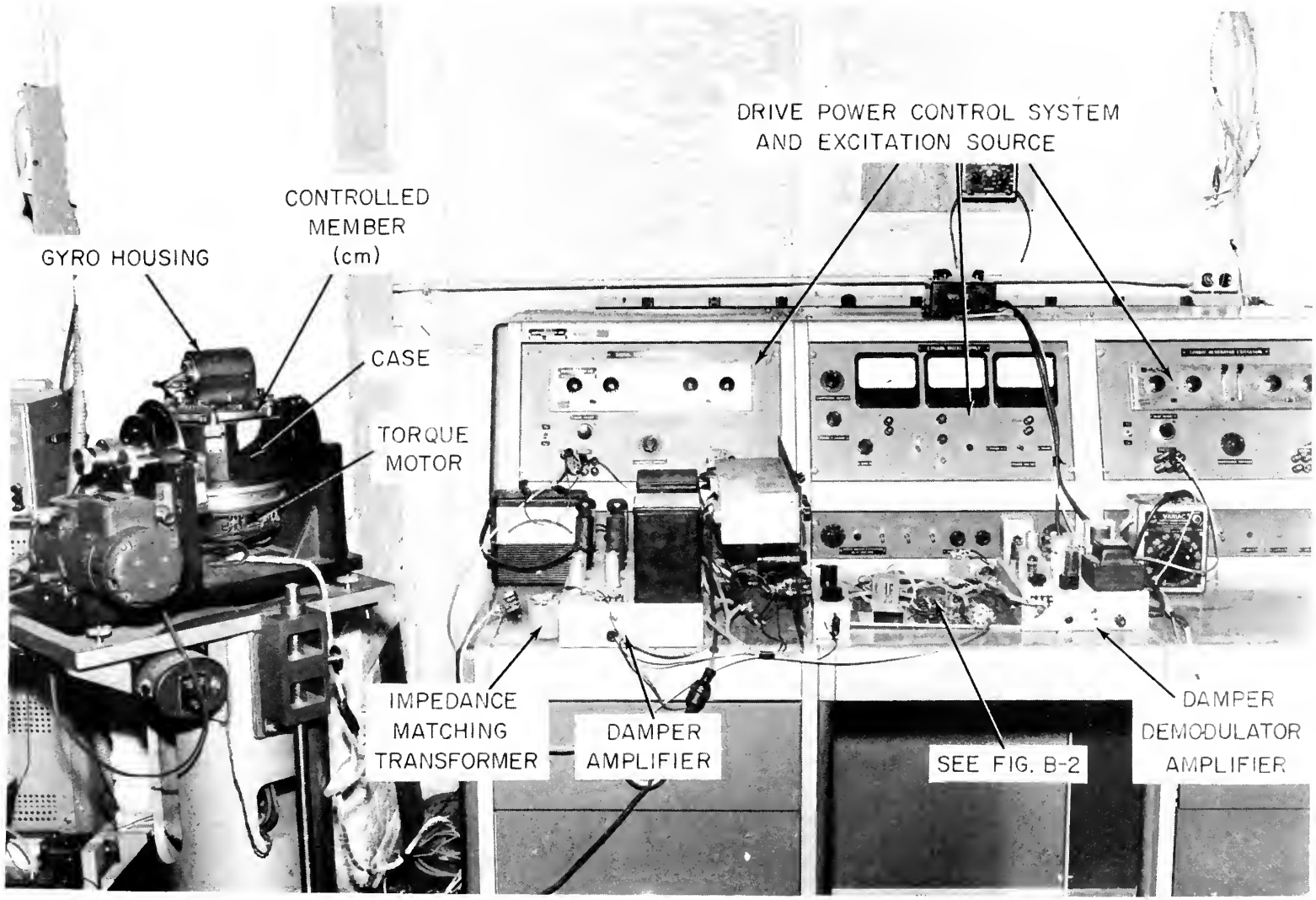

Fig. B-1 Direct-drive stable platform with damping servomechanism

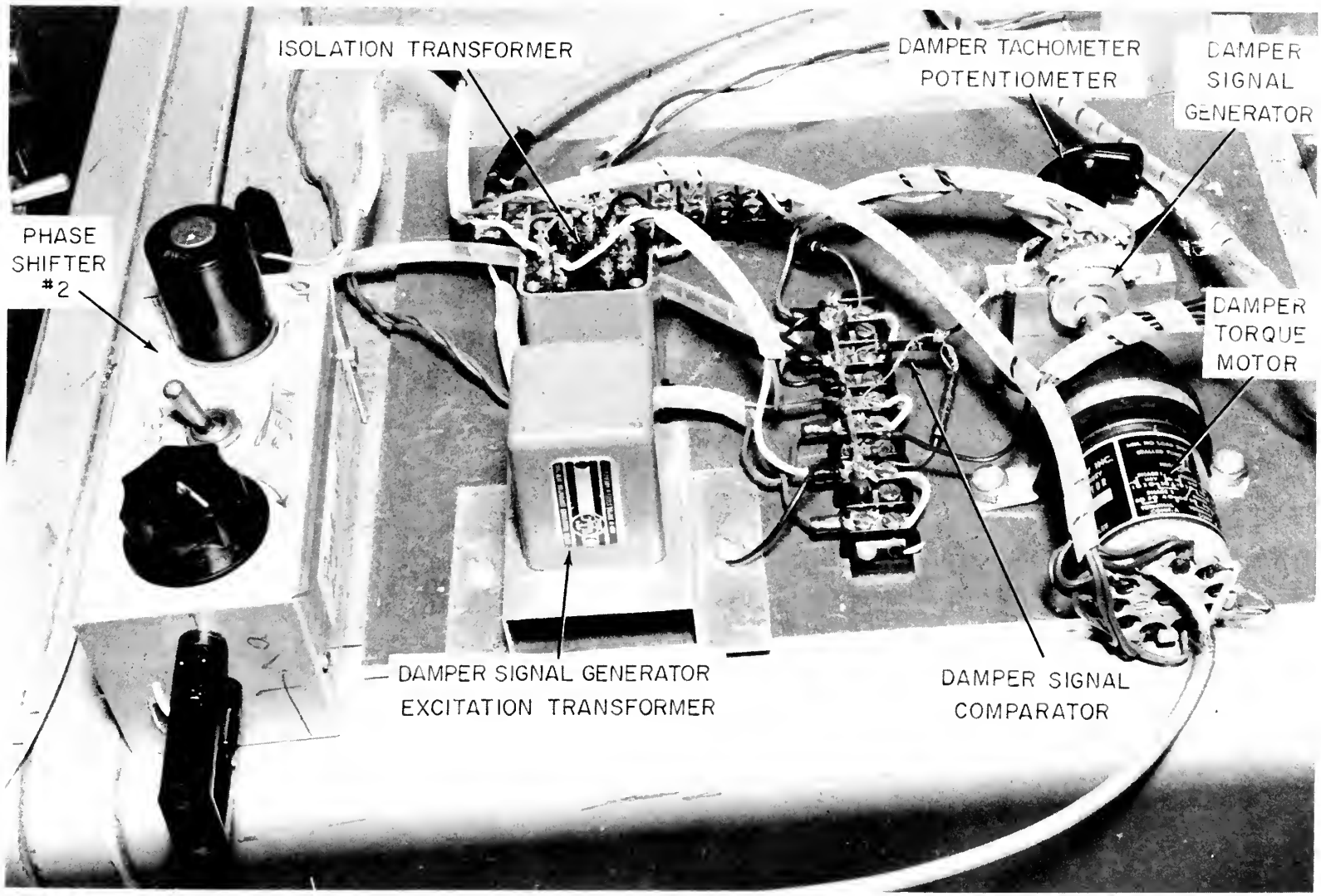

Fig. B-2 The damping servomechanism

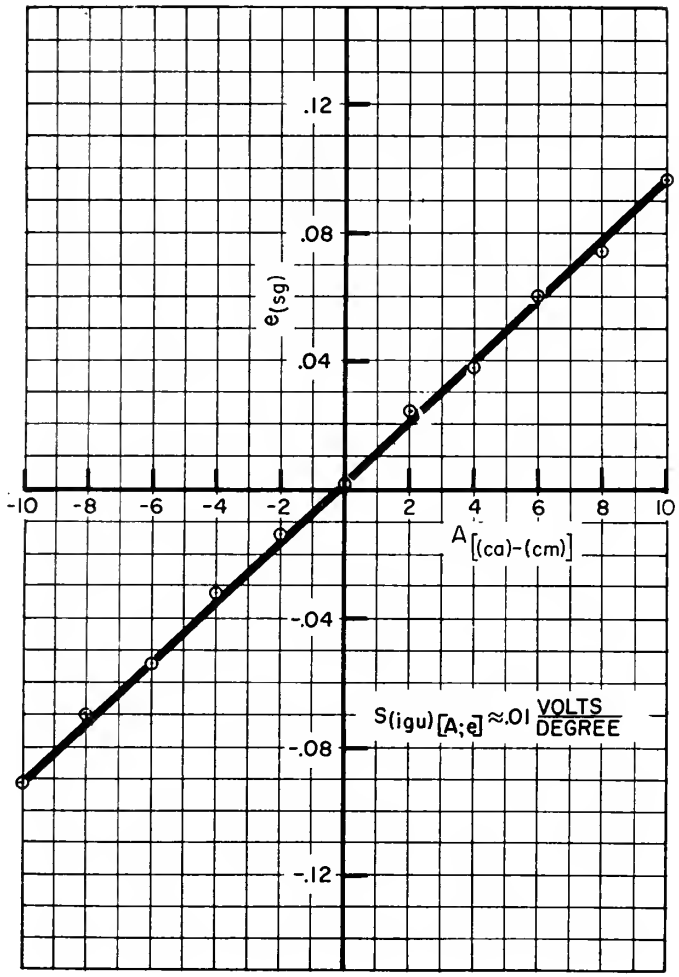

Fig. B-3 Input Angle - Output Voltage of Integrating Gyro Unit

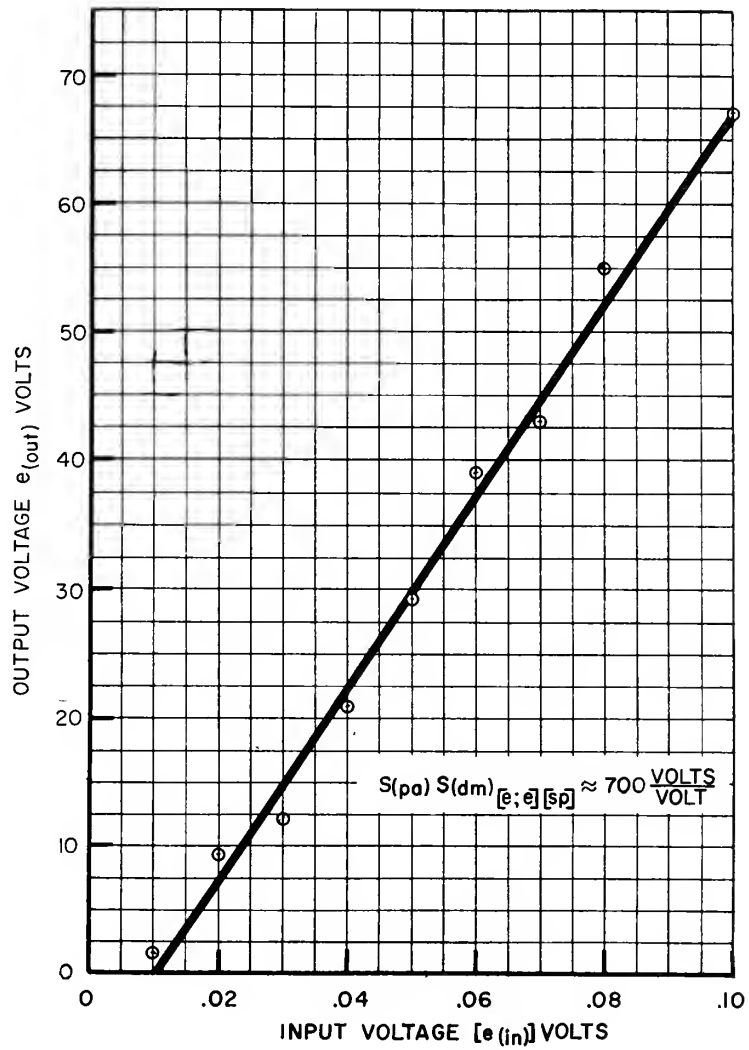

Fig. B-4 Output Voltage vs. Input Voltage for the Preamplifier- Demodulator Combination

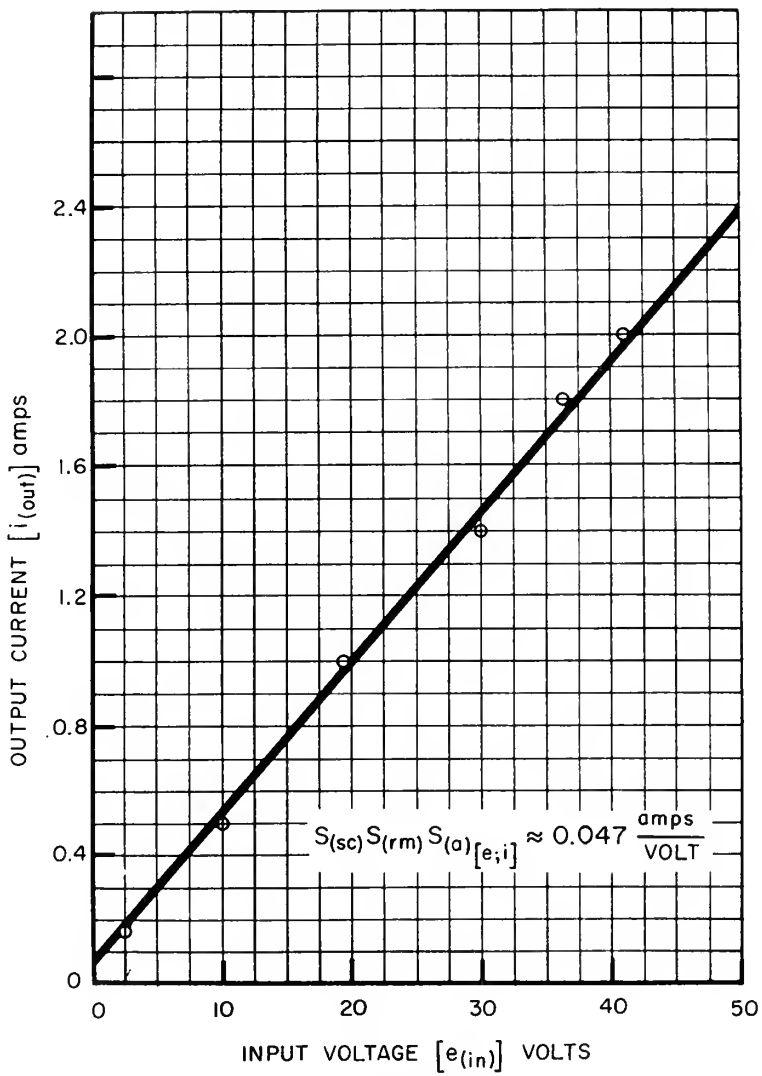

Fig. B-5 Output Current vs. Input Voltage for the Signal Comparator-Remodulator-Amplifier Combination

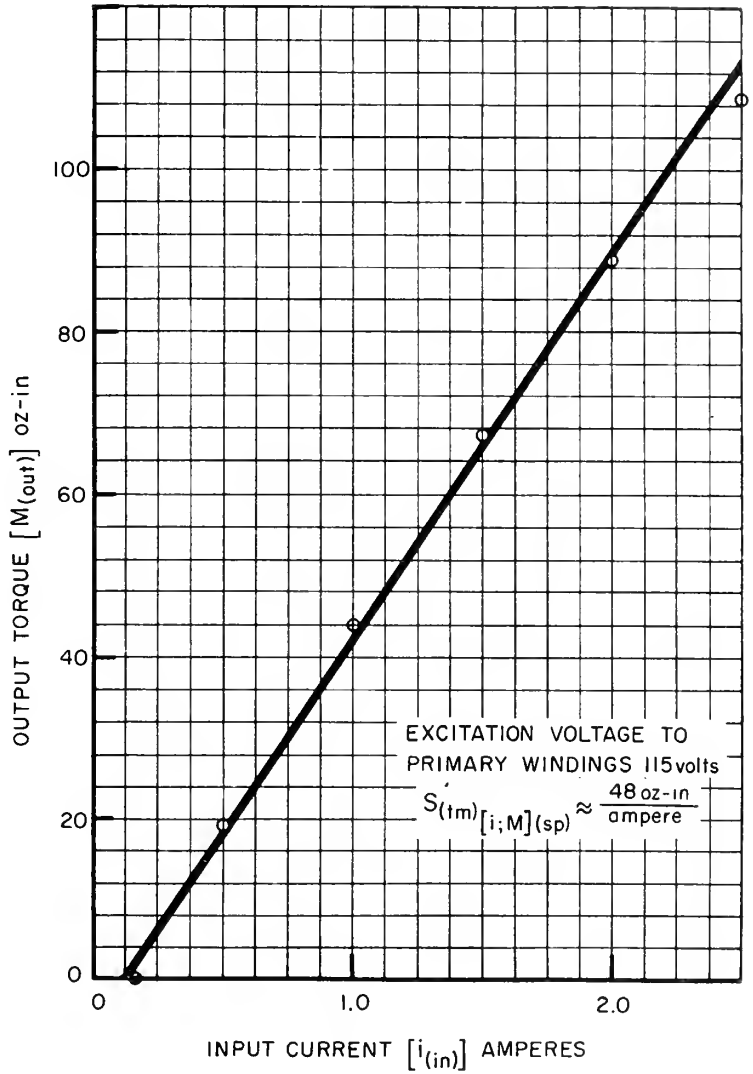

Fig. B-6 Standstill Characteristics of the Stable Platform Torque Meter

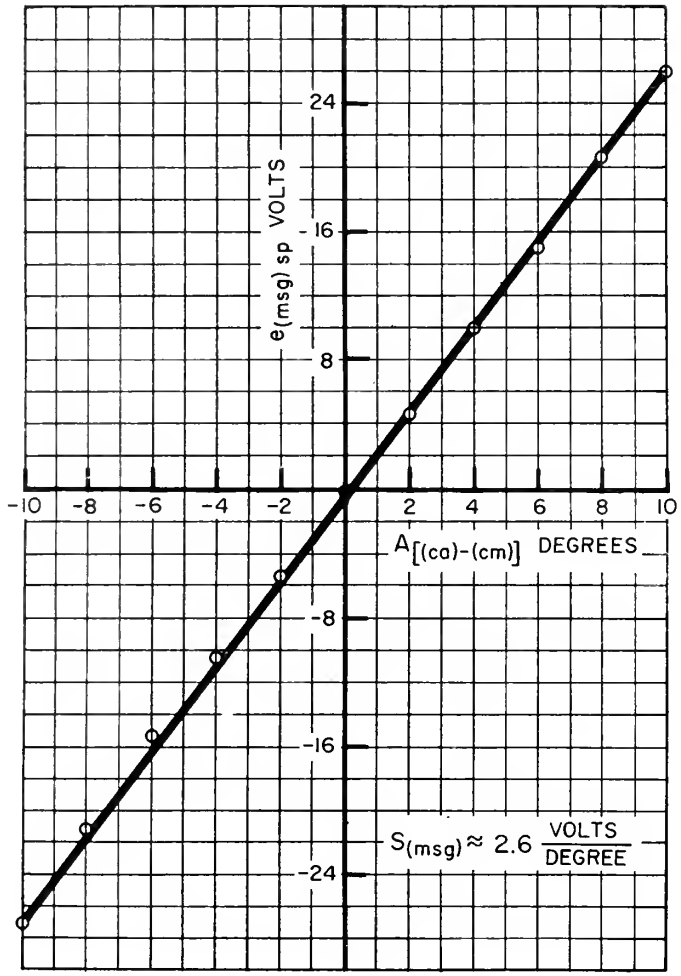

Fig. B-7 Output Voltage - Input Angle for the Microsyn Signal Generator of the Stable Platform

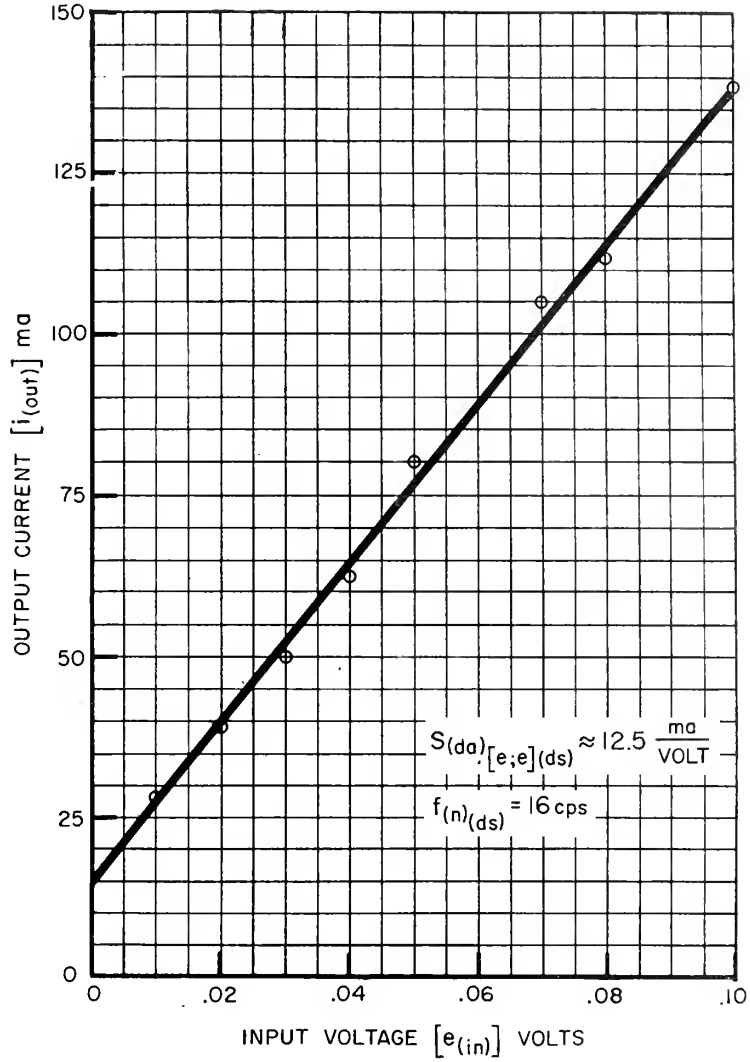

Fig. B-8 Input Voltage - Output Current of Damper Drive Power Control System

parts available at the laboratory. The damping servo system was entirely 400 cps alternating current. All 400 cps power was generated from a single oscillator in the console. However, it was necessary to carefully phase the carrier of the damper signal generator excitation voltage with the carrier of the correction signal voltage in order to insure proper summing in the damper signal comparator. The damper tachometer output was fortunately properly phased.

An isolation transformer and a phase shifter (#1) were installed between the damper signal comparator and the damper torque motor drive amplifier. The phase of the carrier of the signal comparator output voltage was shifted to ninety degrees with respect to the carrier of the damper torque motor excitation voltage.

Two-stage amplification was performed by a high fidelity, Fisher preamplifier, Model 50c and matching 50 watt, power amplifier, model 50A. The maximum output impedance of 16 ohms required the use of an impedance matching transformer.

The damper torque motor and the damper tachometer were contained in one unit, a Kearfott Motor-Generator, R-8001A-A with a stall torque of 1.4 oz. in. The only loads on the motor were the damper tachometer and the damper signal generator.

The damper signal generator was an Electro Mech. Corp., one-turn, ultra low torque potentiometer, 9CJ-10-250. This potentiometer was not center-tapped. A reference ground was provided in the center of the winding of the potentiometer by exciting the potentiometer through a transformer with the center tap of the secondary winding grounded as shown in Fig. B-11.

Undamped natural frequencies up to fifty cycles per sec were obtained in the damping servomechanism. It was estimated that with better design this frequency could be doubled. Only one-third of the rated current of the control windings of the torque motor was used to obtain fifty cycles per second.

The zero frequency characterisitcs of the damping servo system are given in Fig. B-8, B-9, and B-10. The damper tachometer potentiometer sensitivity was set at .0022 volts (rms) ($S_{(dta)\ [A;e]\ (ds)}$ = .0022 volt/(degree). The damper tachometer sensitivity was taken from the Kearfott Components Manual, 1954, as $S_{(dta)\ [A;e]}$ = 0.0296 volts (rms) rad/sec.

The damping servomechanism was constructed by the authors. Optimum configuration and performance were not achieved.

Determination of the Moment of Inertia of the Controlled Member of the Stable Platform

The moment of inertia of the controlled member was determined experimentally in the following manner. The inertia measured included the gyro table, spindle, and torque motor rotor assembly, the integrating gyro and its mounting and associated equipment mounted on top of the table.

From the equation:

$$I\,A_{(cm)} + C\,A_{(cm)} + k\,A_{(cm)} = M_{(in)} \qquad \text{(B-1)}$$

$$I = \frac{k}{\omega_n^2} \qquad \text{(B-2)}$$

The ω_n of the table was determined by recording the transient response of the table with springs mounted on it in such a way to provide an elastic restraint. The damping ratio was determined from the peak to peak ratio curves Fig. 19-4, Vol II, Instrument Engineering, Draper, McKay, and Lees.

$$\omega_n = \frac{\omega_f}{\sqrt{1\ \zeta^2_{(res)}}} \qquad \text{(B-3)}$$

The elastic coefficient of the springs was measured by

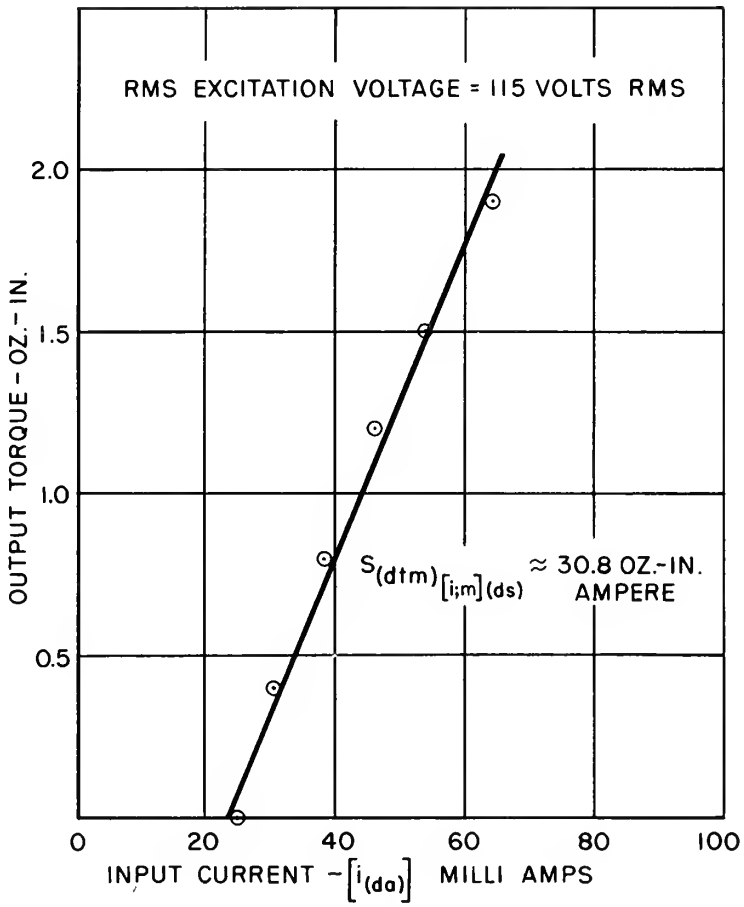

Fig. B-9 Standstill Characteristics of the Kearfott R 800 1A-1 Meter Generator

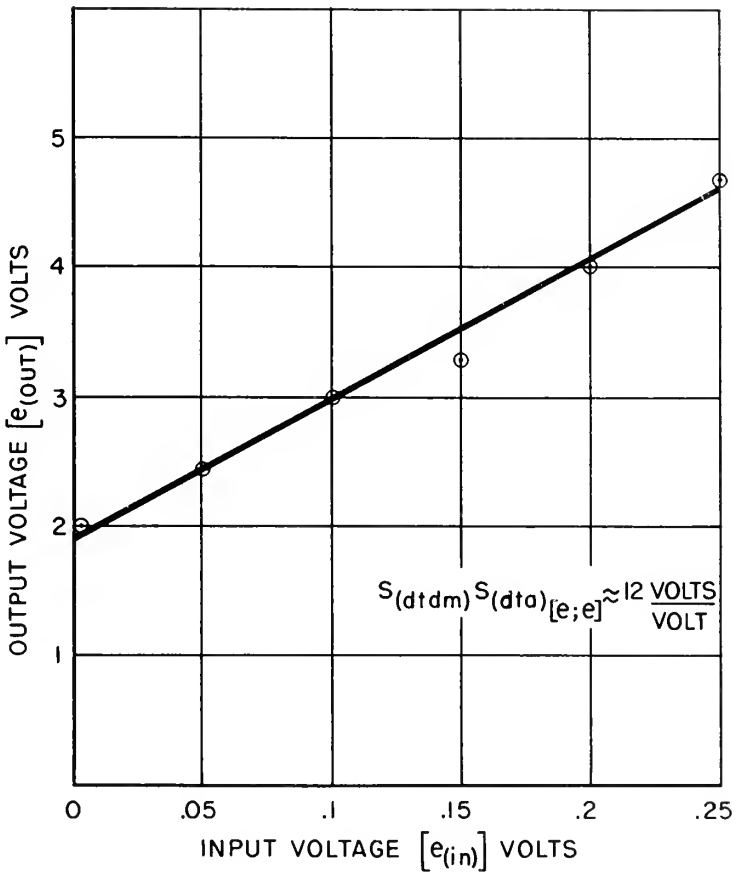

Fig. B-10 Input Voltage - Output Voltage of the Damper Tachometer Demodulator-Amplifier Set at Maximum Gain

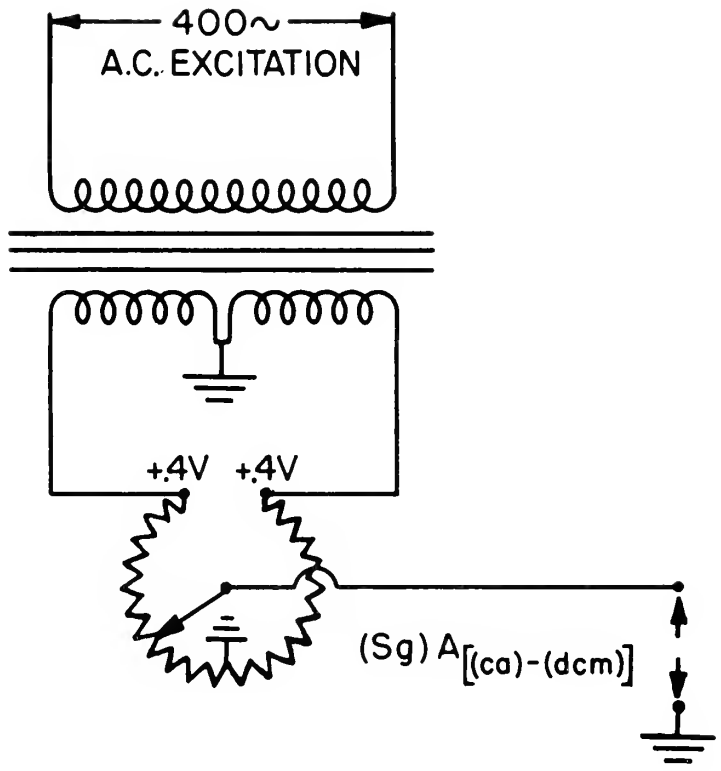

Fig. B-11 Damper Signal Generator and Excitation Transformer

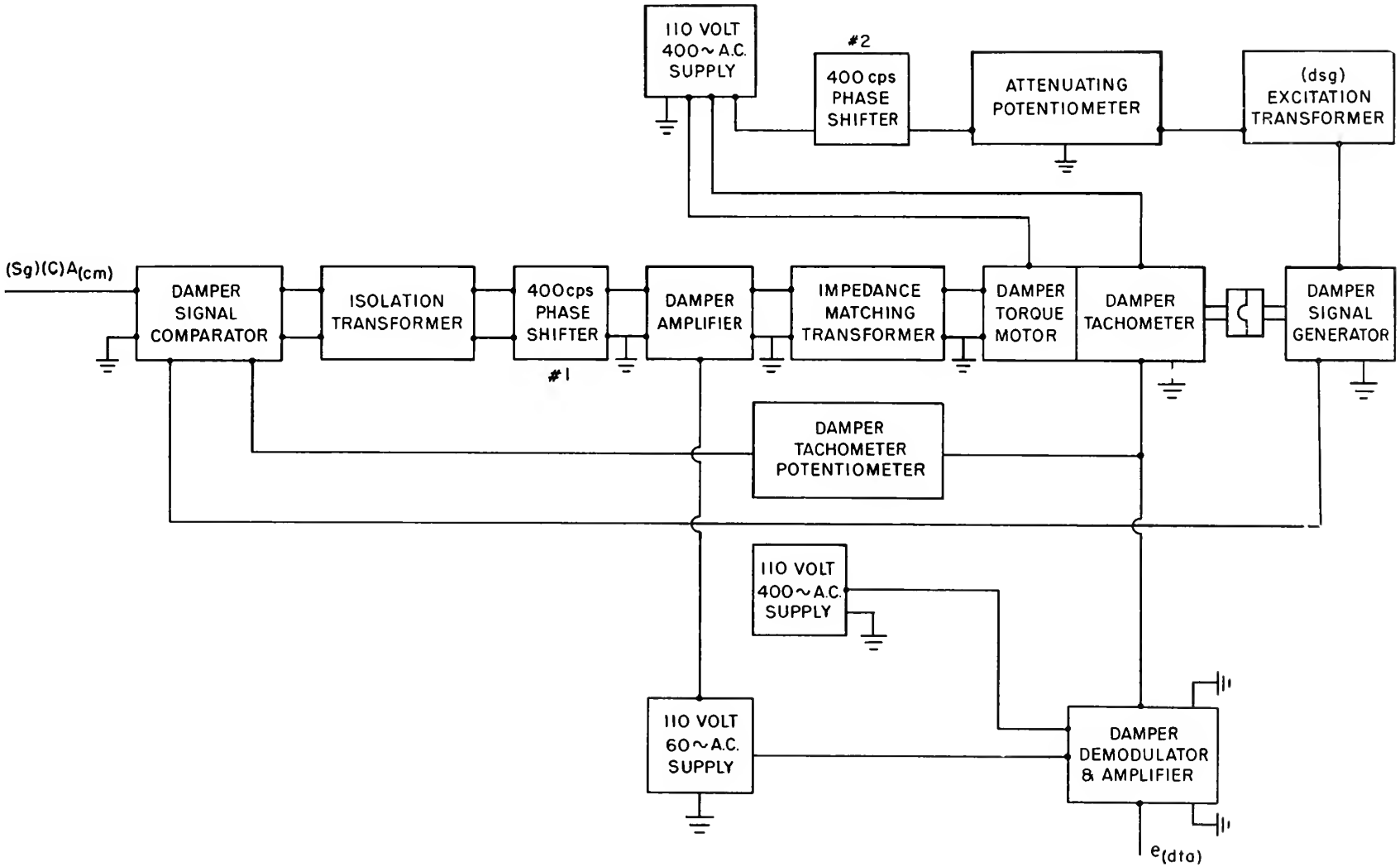

Fig. B-12 Functional Schematic Diagram of Damping Positional Servomechanism

hanging a mass at the end of a wire with low friction pulley such that a torque was put on the table causing an angular displacement from the zero position. A series of points were plotted and the spring constant , k, was determined from the curve.

From equation (B-2) and (B-3) above and the measured values of spring constant and ω_f , $I_{(cm)}$ was computed.

$$k = 94 \times 10^6 \text{ gm cm}^2/\text{sec}^2$$

$$\omega_f = 20.9 \text{ rad/sec}$$

$$\zeta_{(res)} = .045 \text{ (computed)}$$

$$I_{(cm)} = 213 \times 10^3 \text{ gm-cm}^2$$

BIBLIOGRAPHY

1. Draper, C.S. and Woodbury, R.B., Geometrical Stabilization Based on Servodriven Gimbals and Integrating Gyro Units, M.I.T. Cambridge, Mass.

2. Draper, C.S., Wrigley, W., and Grohe, L.R., The Floating Integrating Gyro and Its Application to Geometrical Stabilization Problems on Moving Bases, Sherman M. Fairchild Publication Fund Paper No. FF-13, Institute of the Aeronautical Sciences, New York, Jan. 1955.

3. Lees, Sidney, Design Bases for Multiloop Positional Servomechanisms, Report R-96, Instrumentation Laboratory, M.I.T., Cambridge, Mass, Dec. 1955.

4. Lees, Sidney, Blaschke, T.C., Report R-124, Design Bans for Cascade-Type Positional Servomechanisms, M.I.T., Cambridge, Mass., October 1956.

5. Draper, , McKay and Lees, Instrument Engineering Vol. I, II, and III, McGraw-Hill Publications in Aeronautical Science, 1955.